Document donwnloaded from:

[http://redivia.gva.es/handle/20.500.11939/6684]

This paper must be cited as:

[Asins, M.J., Raga, M.V., Roca, D. et al. (2020). QTL and candidate gene analyses of rootstock-mediated mandarin fruit yield and quality traits under contrasting iron availabilities. Tree Genetics & Genomes 16, 79]

The final publication is available at

[http://dx.doi.org/10.1007/s11295-020-01472-w]

Copyright [Springer]

QTL and candidate gene analyses of rootstock-mediated mandarin fruit yield and quality traits under contrasting iron availabilities

Maria J. Asins*, M. Verónica Raga, Dolors Roca, Emilio A. Carbonell

Instituto Valenciano de Investigaciones Agrarias, Carretera de Moncada a Náquera Km 4.5, Apartado Oficial, 46113 Moncada, Valencia, Spain.

* Corresponding author; email: mjasins@ivia.es Telephone: 34 963424067

https://orcid.org/0000-0002-4330-160X

Abstract

The most sustainable approach to overcome iron deficiency in fruit crops is breeding for rootstocks with a higher capability to acquire iron (Fe) from the soil. The objective of this study was quantitative trait loci (QTL) and candidate gene analyses of rootstock-mediated low-Fe tolerance in terms of fruit yield and quality traits, including Fe fruit content, in a satsuma mandarin-grafted rootstock population derived from a cross between *Citrus reshni* (Cleopatra mandarin) and *Poncirus trifoliata*, under sufficient and low-Fe fertilization (15.3 vs 5.2 µM Fe, respectively).

Iron reduction to one third significantly decreased satsuma leaf chlorophyll concentration, fruit iron concentration, and the fruit/leaf iron proportion. Thirty-four QTLs were detected for 46 heritable traits. Eighteen of them were also found significant when testing each parental genome separately. Seven QTLs contributed to the fruit concentrations of Cu, Fe, K, Na, and S. QTLs involved in rootstock mediated tolerance to Fe deficiency and fruit quality traits distributed into five genomic regions whose gene contents (assuming collinearity with the *C. clementina* genome) were investigated for overrepresented molecular functions and biological processes, and putative functional candidates. Among them, a metal-NA-transporter YSL3 (Ciclev 10019170m), four phytochelatin synthases, an iron-chelate-transporter ATPase, and four basic/helix-loop helix genes coding for likely relevant transcription factors in Fe homeostasis under Fe deficiency were found: bHLH3 (Ciclev10019816m), bHLH137.1 (Ciclev10031873m), bHLH123 (Ciclev10008228m) and ILR3 (Ciclev10009354m). Genes within three QTL regions supported a genetic connection between rootstock-mediated tolerance to Fe deficiency and biotic stresses in citrus.

Keywords: Rootstock breeding, Iron deficiency, *Citrus reshni*, *Poncirus trifoliata*, *Citrus unshiu*, Disease resistance.

Introduction

Iron (Fe) is abundant in the soil but it is usually present in an oxidized form, difficult to be acquired by plants. Besides, in alkaline soils which affects around 30% of the earth, Fe solubility is low leading to iron deficiency chlorosis (Mengel 1994). Iron deficiency causes decreases in fruit yield and quality (Almaliotis et al. 1995). Besides, soil Fe deficiency might decrease fruit Fe content, affecting human nutrition, health and well-being (Rashid and Ryan 2004). Iron sulfate and synthetic chelates are commonly used as iron fertilizers to overcome Fe deficiency (Jessop et al. 1990; Abadia et al. 2004) but they are not fully efficient due to their rapid transformation into an unavailable form in the calcareous soil (Fernandez et al. 2004), and increase orchard management costs. Therefore, the best, cost-effective and sustainable approach is breeding for rootstocks with a higher capability to acquire Fe from the soil. Many citrus rootstocks are limited by their inability to sufficiently extract iron and other micronutrients from calcareous soils (Korcak 1987; Manthey et al. 1994) what has motivated numerous studies on citrus germplasm evaluation for tolerance to low-Fe stress (Castle 1987; Castle et al. 2009; Pestana et al. 2011, 2005). In the greatest effort, Castle et al. (2009) provided the following order of rootstocks in decreasing degree of tolerance: Volkamer lemon/Rangpur/sour orange selections/*Citrus macrophylla*>mandarins and mandarin hybrids>citranges>citrumelos>trifoliate orange.

From the agronomic point of view, tolerance to low-Fe stress should be considered in terms of fruit yield and quality, however this type of evaluation is extremely lengthy and costly due to the long juvenility of trees, and the need to identify nucellar seedlings to be grafted with a commercial variety (Raga et al. 2012, 2016; Huang et al. 2018). These varieties mostly correspond to sweet oranges (Citrus sinensis (L.) Osb), mandarins (mainly Citrus clementina Hort. ex Tan.and Citrus unshiu (Mak.) Marc.), grapefruits (Citrus paradise Macf.), pummelos (Citrus grandis (L.) Osb.), and lemons (Citrus limon L. Burm. f.). Cultivars of all these species are always vegetatively propagated by bud grafting onto a seedling rootstock in order to obtain a more uniform and earlier yielding tree with tolerance to pathogens and well adapted to the local edaphoclimatic conditions. Mandarin fruits are excellent sources of vitamin C, mineral elements and provide two important antioxidant phytochemicals: beta-carotene and beta-cryptoxanthin (Lado et al. 2016). Citrus (2n=18 chromosomes) is mostly cultivated in arid and semi-arid areas, some of them, such as the Mediterranean area, are extensively deficient in iron (Jaegger et al. 2000). The analysis of quantitative trait loci

(QTL) governing rootstock-mediated fruit yield and quality traits under contrasting iron levels would be useful to implement marker-assisted selection schemes in rootstock breeding programs and search for functional candidate genes underlying such QTL.

Trying to understand the molecular mechanisms behind citrus adaptation and tolerance to low-Fe stress, several authors have studied root transcriptional and proteomic differences between iron chlorosis tolerant and susceptible citrus rootstocks under contrasting iron fertilization conditions (Fu et al. 2017, Licciardello et al. 2013, Muccilli et al. 2013), the metabolic and molecular changes that take place in citrus under iron deficiency (Martinez-Cuenca et al. 2013, Fu et al. 2017), and recently, Zhang et al. (2020) have provided a reduced list of 14-21 members of the basic/helix-loop-helix (bHLH) transcription factor family as putative key regulators of the iron deficiency response in *C. grandis*.

Here we present a pioneering genetic study of rootstock effects on a grafted mandarin using a *Citrus* × *Poncirus* population. The objectives were the QTL and candidate gene analyses of rootstock-mediated low-Fe tolerance in terms of fruit yield and quality traits, particularly fruit iron content, using a progeny derived from two well-known citrus rootstocks, Cleopatra mandarin (*Citrus reshni* Hort. ex. Tan.) and trifoliate orange (*Poncirus trifoliata* (L.) Raf.) which were previously reported to differ in tolerance to low-Fe stress (Castle et al. 2009). The segregating population was originated by nucellar-seedling propagation from 62 apomictic hybrids of a reference population (151 hybrids) that had been previously genotyped (Raga et al. 2012). In the present study we have anchored an integrated *C. reshnni-P. trifoliata* genetic linkage map to the physical map of *C. clementina*, the most closely related species to *C. reshni* (Herrero et al. 1996) whose sequence is available, to approach an intensive candidate gene analysis within relevant QTL regions taking advantage of citrus databases (phytozome.jgi.doe.gov, citrus.hzau.edu.ch, ncbi.nlm.nih.gov) and bioinformatic tools.

Materials and Methods

Plant material

A mapping population that consists of 151 hybrids (R×Pr) previously genotyped (Raga et al. 2012) was used to identify apomictic hybrids (Raga et a. 2016) that were propagated through nucellar seedlings and grafted for the present experiment. The process and steps towards the obtention of both mapping and phenotyped populations are graphically described in Figure 1. The mapping population was obtained at IVIA (Valencia, Spain) by controlled crosses between *Citrus reshni* Hort. ex. Tan. (Cleopatra

mandarin) as female (salt and iron chlorosis tolerant and apomictic) parent, and two apomictic and disease resistant varieties of *Poncirus trifoliata* (L.) Raf. (trifoliate orange): Flying Dragon (83 hybrids) and Rich (68 hybrids) as pollinators. Seedlings of the next generation were analyzed by molecular markers to discard the zygotic ones (Ruiz et al. 2000). Finally, nucellar seedlings obtained from the 62 R×Pr hybrids that showed apomictic reproduction and parents (Cleopatra and Flying Dragon) were grafted with Clausellina mandarin (*Citrus unshiu* (Mak.) Marc.) and maintained for more than 5 years till full production before the experiment.

Growth conditions

Two-Three out of six repetitions (nucellar grafted plants) of each R×Pr hybrid were randomly selected to establish two treatments: control-sufficient (15.3 μM Fe) and low-Fe treatment (5.2 μM Fe), during 9 months (from February till November) in a greenhouse. Plants were growing into pots (17 L) using cocofiber as a substrate. The greenhouse had automatic roof ventilation and heating system (maintaining inside air temperature above 8°C). A high frequency fertirrigation system together with 4L/h drippers were used and handled to ensure homogeneity of low [Fe] at the roots of all plants in cultivation at the same time. The nutrient solution (pH: 6.4) contained the following concentration of macronutrients (in mM): NO_3^- 8.1; $H_2PO_4^-$ 4; SO_4^{2-} 1; NH_4^+ 0.9; K^+ 4.2; Ca^{2+} 3.5; Mg^{2+} 1; plus, the following concentration of micronutrients (in μM): Mn^{2+} 8; Zn^{2+} 2.3; B 20, Cu^{2+} 7; Mo^{4+} 0.5 and Fe^{2+}15.3 or 5.2 depending on the treatment (control or low-Fe, respectively). The water for the nutrient solution was previously treated with reverse osmosis.

Trait evaluation

Several vegetative, physiological and agronomic (related to fruit yield and quality) traits were evaluated on the grafted satsuma variety (see Table 1 for the abbreviation list) under both control and low-Fe conditions, denoted by C_ and Fe_ prefixes, respectively. Chlorophyll leaf concentration of fully expanded young leaves from each plant (S3) was estimated with the chlorophyll meter SPAD-502 Plus (Konica Minolta, INC., Japan) after 3 months of treatment. Three fully developed leaves per plant were sampled from vegetative spring shoots after 8 months of treatment to measure the following leaf characteristics: leaf fresh weight (LFW, g); leaf dry weight (LDW, g) measured in samples dried at 80°C for 3 days, leaf water content (LWC, g) as the difference between fresh and dried weights, leaf dry matter (LDM, %) calculated

as the percentage of LDW to LFW, and Leaf area [LA (square centimeter)] measured with a leaf area quantifier (LI-3100C area meter; LI-Cor, Lincoln, NE).

A minimum of 5 randomly sampled fruit per tree also were evaluated for the following internal fruit-quality traits: fruit weight (FW, in g); fruit diameter (FD, in mm); rind thickness (RT, in mm); juice volume per fruit (JV, in mL) without pulp, juice content (JC, percentage from JV and FW), soluble-solids content [SSC, as º Brix, using a digital refractometer (Pallete PR-101; Atago, Tokyo, Japan)], juice acidity measured as volume of NaOH 0.1 M to neutralize acidity per fruit (NaOH, in mL, using phenolphthalein indicator), and maturation index (SSC/A, as the ratio between SSC and the percentage of citric acid calculated from NaOH).

Dry tissue samples of the fruit raw edible part (F), and leaf (Lf), were prepared for mineral analysis by digestion in a HNO_3:$HClO_4$ (2:1, v/v) solution. Inorganic solutes were determined in ppm (mg/Kg) by inductively coupled plasma spectrometry (Varian ICP 720-E, Scientific Instrumentation Service, Estación Experimental del Zaidín, CSIC, Granada, Spain). These traits were named by the element symbol followed by F or Lf, denoting the tissue. Inorganic solutes were also determined in the leaf at the beginning of the low-Fe treatment. Thus, the change (accumulation or loss) of each element concentration, denoted by the prefix d, was estimated as the difference between its final and initial leaf concentrations. The relative Fe_F to Fe_Lf was also considered (Fe_F/L) as percentage, and also the relative Al_F to Al_Lf (Al_F/L).

Fruit yield was evaluated in terms of number of normal, ripe fruits (FNm), their individual weight, (FWm, g) and total fruit weight (TFWm, Kg). Total dry fruit weight (TDFWp, g) was estimated from the mean dry weight of fruit pulp and FNm, Finally, total harvested Fe (mg of Fe in total fruit yield) was deduced from TDFWp and Fe_F. This trait, coded as FeUEp, could be considered as a comparative, agronomic indicator of the rootstock iron uptake and translocation capacity, under both Fe levels (Asins et al. 2020). Similar estimations for P, S and Mg fruit contents (PUEp, SUEp and MgUEp) were also obtained.

Statistical analysis

Pearson correlation coefficients and principal component analysis based on the correlation matrix for the adjusted means were used to study the relations between the different traits.

The experiment was designed as a split-plot with four blocks using iron treatments as the main plot and rootstocks as the subplots. The statistical analysis of the

experiment followed this experimental design, i.e. blocks were random, and to study the G×E interaction the effects of genotype and treatment were classed as fixed. Considering R×Pr hybrid genotypes as a random effects factor, broad-sense heritability (H^2) was estimated for all traits for nucellar rootstocks (repetitions) derived from apomictic R×Pr hybrids under control or low-Fe conditions, based on the genotypic (V_G) and environmental (V_E) variance estimators calculated by minimum variance quadratic unbiased estimator (MIVQUE), as previously reported (Villalta et al. 2007).

Molecular markers, QTL and candidate gene analyses

QTL analyses were carried out using the genotypic and map data from Raga et al. (2012) based on SSR, IRAP and SCAR markers, and the adjusted means of traits. Interval Mapping (IM) procedure in MapQTL ® 6 (Van Ooijen 2009), and Multiple QTL Mapping (MQM) when more than one QTL was detected in the same linkage group were used to identify QTLs. QTL analyses were carried out in two different ways. First, we analyzed the data as a cross-pollinated (CP) population type in order to consider intralocus interaction and second, we analyzed data for each parental meiosis separately; i.e. a "two-way pseudo-testcross" analysis (Grattapaglia and Sederoff 1994). This second approach provides the computation advantages of the two-genotypes QTL model but the disadvantage of losing power (and reality) because intralocus interaction is ignored (Van Ooijen 2009). JoinMap 4.1 (Van Ooijen 2012) was used to translate and split the marker data to separate the two meiosis. Some linkage groups or linkage group parts (R9a, R6, R4a, Pr1, Pr4a, and Pr9b) were parent-specific; so they were ignored when using the CP data for QTL analysis. Cleopatra map contained 86 markers, distributed along 10 linkage groups, covering 1127.127 cM of the *C. reshni* genome. Similarly, *Poncirus* map contained 73 markers, distributed along 11 linkage groups, covering 1416.759 cM of the *Poncirus trifoliata* genome. The CP map contained 93 markers, distributed along 9 linkage groups, covering 1406.761 cM of the integrated genome.

For IM and MQM, a 5% experimentwise significance level was assessed by permutation tests. These LOD critical values ranged from 1.1 to 2.0 depending on the trait and linkage group in the "two-way pseudo-testcross" analysis (population type DH). On the other hand, the LOD critical values ranged from 2.2 to 3.3 depending on the trait and linkage group in in the CP analysis. Only significant QTLs with LOD≥2.38 for heritable traits ($H^2>0$) are reported here.

A two-way ANOVA was used to study the interaction (epistasis) between markers corresponding to QTLs controlling some traits (Fe_Cu_F, Fe_S3 and Fe_FeUEp).

Some genomic regions were particularly rich in QTLs or had QTLs for relevant traits. For these regions, markers from the CP map were anchored to the physical map of *C. clementina* using primer and/or EST sequences and the BLASTN tool (https://phytozome.jgi.doe.gov/pz/portal.html#!search?show=BLAST). Genes covering one LOD decay at both sides of the QTL peaks were downloaded from *C. clementina* genome at https://phytozome.jgi.doe.gov. *C. clementina* was chosen instead of *C. sinensis* because Cleopatra mandarin is genetically closer to *C. clementina* than to *C. sinensis* (Herrero et al. 1996, Wu et al. 2018). The annotation of some genes downloaded from phytozome.jgi.doe.gov was tested by blasting their peptide sequence at ncbi.nlm.nih.gov. Gene ontology (GO) enrichment analysis of genes within one LOD intervals of QTLs were carried out using the Singular Enrichment Analysis tool (Tian et al. 2017) at the AgriGo platform (http://systemsbiology.cau.edu.cn/agriGOv2/).

Results

The mean (and standard error) of the phenotypic values of controls (Cleopatra mandarin and Flying Dragon parents) for the analyzed traits under Fe-sufficient and low-Fe treatments are presented in Table 1. Significant differences between the parents were detected for a few traits under one Fe level, particularly for S3 (SPAD) under low-Fe treatment (Online Resource 1) where Clausellina leaves grafted on Flying Dragon showed higher chlorophyll content than those on Cleopatra (73.90±1.70 *versus* 49.25±18.85, respectively, in Table 1). The pulp of Clausellina mandarin fruits was found particularly rich in K, followed by P, Ca and S. Silicon was also present and its amount was similar to that of iron for the parental rootstocks under low-Fe stress (20.14±5.04 and 19.32±0.64 ppm, for Cleopatra and Flying Dragon, respectively). Although with the least concentration, aluminium was present in the fruit, particularly under low-Fe condition for Cleopatra (6.96±4.9 ppm).

The range of variation in the grafted rootstock-segregating population and the estimated heritabilities under sufficient (H^2_C) and low-Fe fertilization (H^2_Fe) are also included in Table 1. Heritability estimates of some traits (Cu_F, K_F, P_F, Fe_Lf, Na_Lf, fruit juice tritable acidity (NaOH), TDFWp and related traits), notably increased under low-Fe.

A summary of results from the mixed model analysis of the segregating population is provided in Online Resource 2. Leaf [Ca] was the only trait where significant G×E interaction was detected in the experiment. Iron reduction to one third significantly decreased leaf chlorophyll concentration (S3), fruit iron concentration (Fe_F) and the fruit/leaf iron proportion (Fe_F/Lf) (Online Resource 2, Figure 2).

The relationships among traits evaluated under control and low-Fe are graphically represented in Figures 3 and 4, respectively. As expected, most fruit yield traits form a group of strong positive correlations, and negatively related to the group formed by FW and JV. Fruit concentrations of S, K and P are also strongly related forming a conserved group between treatments. Fruit yield traits FNm, TFWm, TDFWp, and PUEp were significantly correlated under control and low-Fe, as well as leaf concentrations of Al, K, Mg, P, S and Si (Online Resource 3). Additional information on significantly ($p<0.02$) correlated traits is given in Online Resource 4. The only elements whose concentrations in leaf and fruit were correlated under both treatments were Na and Mn (P, only under control condition). In the case of Mn, this correlation increased from 0.38 (control) up to 0.63 (low-Fe). Noteworthy, TDFWp and Fe_F were negatively related only under control conditions.

Main features of the 34 significant QTLs detected for 46 heritable traits are shown in Table 2. Eighteen of those QTLs were also found significant when testing each parental genome separately: 11 at the Cleopatra mandarin map, and 7 at the *Poncirus trifoliata* map. Except for fruit yield QTLs FNm and TFWm on linkage group 4b, that were detected under both treatments, the rest are condition-specific. Several rootstock QTLs were found to contribute to the fruit concentrations of Fe and K under control, and of Cu, Na and S under low-Fe fertilization. Epistatic interactions were detected for two traits: Cu fruit concentration under low Fe (between Fe_Cu_F QTLs markers CR17,300 and C8iC1rt,650; Figure 5A), and SPAD values under low Fe (between Fe_S3 QTLs markers CT19.165 and C1,1600; Figure 5B). In all of them, one of the genotypic combinations should be avoided through selection in rootstock breeding programs.

Five genomic regions, four of them showing clustering of QTLs were further analyzed for candidate genes (Table 2 and Figure 6). For this purpose, all markers at these QTL regions were first anchored at the *C. clementina* physical map. A QTL for fruit concentration of Cu was at region I on LG 7 (Scaffold 3); Fruit yield QTLs FNm, and TFWm formed a cluster (IV) on LG 4b (Scaffold 7); and Fe, Mg, S, and P total fruit

contents under low-Fe formed a cluster (II) on LG 7 (Scaffold 3) and another (III) on LG 12 (Scaffold 4). Cluster V corresponded to QTLs for S3, and leaf change of K and Cu concentrations on LG 3b (Scaffold 1). Physical distances in Mbp around the QTL peaks (around 1 LOD) were estimated to download the genes (mRNA) included. Enrichment analysis of these genes resulted in significant Biological Processes for clusters II (signaling), IV (DNA damage checkpoint), and V (phosphorylation, cell recognition); and significant Molecular Functions for regions I (nutrient reservoir activity, GO:0045735, FDR=0.026), II (peptidase inhibitor activity), IV (ADP binding, ATPase activity), and V (protein Ser/Thr kinase activity) (Online Resource 5).

A summary list of candidate genes is shown in Online Resource 6. Among them, a metal-NA-transporter YSL3 (Ciclev 10019170m) was found within cluster II, four phytochelatin synthases were within region I, and an iron-chelate-transporter ATPase in cluster IV. Four basic/helix-loop helix genes coding for likely relevant transcription factors in Fe homeostasis under Fe deficiency (Zhang et al. 2020) were found in clusters I (bHLH3, Ciclev10019816m), III (bHLH137.1, Ciclev10031873m), and V (bHLH123, Ciclev10008228m; and ILR3, Ciclev10009354m). Some genes related to phytohormone metabolism/signaling were found within cluster I (ethylene, auxin), II (ethylene), III (ethylene, polyamines, salicylic acid, auxin), IV (ethylene, gibberellin, brassinosteroid) and V (auxin). Numerous genes annotated as Fe-containing proteins, transporters, channels or exchangers were also found within these genomic regions.

Discussion

QTL analysis of rootstock-mediated scion traits using Citrus × Poncirus progenies

In spite of the importance of the rootstock in citriculture, up to our knowledge, no genetic analysis of rootstock effects on fruit traits has been reported yet. Two well-known reasons are the long juvenility of *Citrus* × *Poncirus* hybrids and the segregation for apomictic reproduction in these populations (Raga et al. 2012). Thus, although the present study is based on a genetic linkage map previously obtained from the whole *C. reshni* × *Poncirus trifoliata* progeny (151 trees; Raga et al. 2012), only 62 showed the needed apomictic reproduction to be used as rootstock (Fig. 1). Therefore, a limitation of this study is the number phenotyped genotypes because not all of them could be replicated through nucellar seedlings and grafted for phenotypic evaluations. Under this circumstance, QTL resolution is not limited by marker density but by the size of the phenotyped subpopulation. Recent QTL studies in *Citrus* × *Poncirus* segregating

populations (Lima et al. 2018; Huang et al. 2018) have used saturated linkage maps, mostly based on SNPs, for each parent and the double pseudo-testcross mapping strategy (Grattapaglia and Sedoroff 1994). This strategy only allows the detection of allele-substitution effects at each parental genome which is less powerful for QTL detection than the cross-pollinated (CP) model, and too abstract for practical use in breeding programs. Instead of SNPs, using SSR, IRAP and SCAR markers has allowed us the detection of up to the four possible genotypes (ac, ad, bc and bd) segregating in a *Citrus* (ab) × *Poncirus* (cd) progeny, in some genomic regions, and the use of the CP model (instead of the pseudo-testcross strategy) resulting in the gain of power in the QTL detection (Van Ooigen 2009). Thus, 16 out of 34 QTLs in Table 2 were not detected using the pseudo-testcross strategy, indicating they would correspond to intralocus interactions in the CP model. This model is more realistic and useful for breeding purposes. Besides, intralocus interactions may be molecularly important in citrus. Thus, Jiao et al. (2013) found that 11.7% of heterozygous genes in *C. sinensis* were differentially expressed. Then, it could be reasonable to expect a higher percentage of differentially expressed heterozygous genes in *C. reshnii* × *Poncirus trifoliata* hybrids given the large genetic distance between their parental species (Herrero et al. 1996).

Another limitation of the present QTL analysis is the limited extent of integrated or consensus *Citrus-Poncirus* linkage groups, not due to the progeny size (151) but more likely to the cytogenetic differences that exist between *C. reshnii* and *P. trifoliata* (Barros et al. 2010, Mendes et al. 2011).

Taken together both limitations, the size of the phenotyped progeny and the extent of *Citrus-Poncirus* linkage groups, they explain the low number of the QTLs detected in this study and the scarcity of common QTLs between treatments (2), although most traits were not globally affected by the treatment (Table 1). In general, more QTLs were detected under low-Fe than control conditions, in agreement with the differences in trait heritabilities between treatments.

Rootstock effects on fruit quality traits and the effect of lowering external Fe nutrition.

In the case of mandarin fruits, the allocation of minerals (fruit *vs* leaf) is important regarding human health and nutrition. Results on Clausellina fruit concentration of elements (Table 1) generally agree the ranking reported in previous studies (Lado et al. 2016; Czech et al. 2020; Hong et al. 2018); however, there are two

remarkable differences: the presence of Si, particularly when using the parents as rootstocks, and the relative amount of Sulphur, the fourth element regarding concentration. These are good news. Sulfur is an essential dietary mineral primarily because amino acids contain it. Sulphur is thus considered fundamentally important to human health, and conditions such as nitrogen imbalance and protein-energy malnutrition may result from its deficiency. The detection of rootstock QTLs controlling the fruit concentration of mineral elements (Fe, K, Cu, Na and S), maturation index (C_SSC/A), and fruit juice acidity (Fe_NaOH) in the present experiment (Table 2) supports the hypothesis that rootstock genotype is contributing to the level of some nutrients in the fruit, such as it was also found in tomato (Asins et al. 2020). Therefore, those mandarin quality traits could be improved through rootstock breeding programs.

In general, leaf concentrations of elements are highly correlated between Fe treatments what it is not the case in fruit except for Si (Online Resource 3). Lowering the external iron input significantly affected S3, Fe_F and Fe_F/Lf (Online Resource 2, Fig. 2) suggesting less iron is moved (partitioned) towards the fruit what might be seen as the consequence of a regulatory process induced by the plant sensing. If we reduce this sensitivity through the rootstock, we might be able to maintain crop yield and, at the same time, fruit iron content, lowering fertilization costs. Other changes related to the trait correlations were observed. Under low-Fe, Fe_F is positively related to Cu_F, Mn_F, Ca_F, FeUEp and S3 (Online Resource 4, Fig. 4). From these traits, Fe_F was only significantly related to Mn_F and Ca_F under control conditions where it was found negatively related to TDFWp and FNm (Fig. 3). These findings suggest that Fe_F is limited by the total dried pulp weight yielded only under control conditions (the more TDFWp, the less Fe_F), while under low-Fe, the iron fruit concentration appeared as the main trait (lowest p-value) related to the status of photosynthesis machinery (measured by SPAD value, S3). Decreases in S3 with Fe deficiency have been previously observed in different plant species, including fruit trees such as peach and citrus (see Martinez-Cuenca et al. 2013). The parents of the rootstock segregating population were significantly different for S3 (Online Resource 1) under low-Fe where, unexpectedly, Flying Dragon (*Poncirus trifoliata*) behaved as more tolerant than Cleopatra. *P. trifoliata* is usually considered more susceptible to iron chlorosis than Cleopatra (Castle 1987). This disagreement in the ranking might be due to differences in the treatment to induce low-Fe availability at the root (rising pH *vs* decreasing [Fe] of

nutrient solution), and/or intraspecific genetic and agronomic diversity within the species *P. trifoliata* (Fang et al. 1997, Ben Yahmed et al. 2016, Huang et al. 2018). Two QTLs were detected for S3, only under low-Fe; one of them, on LG 10+5b was also detected in the corresponding LG of Cleopatra. Given that both QTLs were epistatic (Figure 5B), this interaction has to be considered to select the best (tolerant) genotype combination (**ac** at CT19.165, and **lm** at C1,1600).

Candidate gene analysis

The causal relationship between variation of an agronomic trait and genotypic differences is important for developing targeted strategies in molecular breeding (Varshney et al. 2014). Therefore, any functional or bioinformatics analysis to allow priorization of candidate genes in QTL regions is valuable to guide further experimentation and validation of causal genes underlying QTLs (Bargsten et al. 2014). The clustering of QTLs involved in rootstock mediated tolerance to iron deficiency and fruit quality traits in five genomic regions led us to investigate their gene contents (assuming collinearity with the *C. clementina* genome in these regions), looking for molecular functions and biological processes that were more frequent than expected (i.e. overrepresented), and putative functional candidates. Thus, the genomic region I containing a QTL for fruit concentration of copper was particularly rich in nutrient reservoir activity. This region contains numerous germin-like proteins and all annotated glutathione gamma-glutamylcysteinyltransferases (Online Resource 6) which are involved in the synthesis of phytochelatins, the heavy-metal-binding peptides of plants (Ramos et al. 2007).

Citrus-Poncirus genomic regions containing clusters II and III were particularly relevant for the total fruit content of Fe and other nutrients (S, P, Mg) under low-Fe stress (Figure 6, Table 2). Among numerous transporters, a metal-nicotianamine transporter YSL3 (Ciclev10019170m) is within cluster II. Yellow Stripe-Like (YSL) family of proteins are transporters of metals that are bound to the metal chelator nicotianamine or the related set of mugineic acid family chelators known as phytosiderophores. In Arabidopsis, AtYSL1 and AtYSL3 are localized to the plasma membrane, function as iron transporters (Chu et al. 2010) and are regulated in response to the Fe status of the plant (Waters et al. 2006). In citrus roots, Fe deficiency promoted the expression of a PAL gene and the accumulation of phenolic compounds what could promote Fe solubilization (Yang et al. 2016). A gene coding for PAL is located in cluster III, and a gene coding for transcription factor MYB 54, required to activate the

expression of PAL in Arabidopsis (https://www.uniprot.org/uniprot/Q9LK95) is in cluster II. As a result of Fe deficiency, Martinez-Cuenca et al. (2013) found increased citrate and malate concentrations in xylem sap and root exudates of Carrizo citrange and this was concomitant with the differential expression of several enzymes related to their metabolism. Genes coding for glutamate decarboxylase, malate dehydrogenase, pyruvate kinase, and dihydrolipoyllysine-residue acetyltransferase component 1 of pyruvate dehydrogenase complex were found within clusters II and III (Online Resource 6). Besides, a gene coding for phosphoenolpyruvate carboxylase 1 (Ciclev100014164m) is within the QTL interval for Fe_S3 on linkage group 10+5b.

Genes involved in oxidative stress response have been frequently reported to be differentially expressed in citrus roots as a consequence of Fe deficiency (Forner-Giner et al. 2009, Licciardello et al. 2013, Muccilli et al. 2013). Two Fe-Mn superoxide dismutases, several glutathione-S transferases, and a thioredoxin and a ferredoxin (Ferredoxin-Thioredoxin system), were found within cluster III. A great deal of evidence has shown that numerous environmental factors and pathogens can induce ROS generation in plant cells (Huang et al. 2019).

Regarding transcriptional regulation, four genes coding for bHLH transcription factors that could play a relevant role in Fe homeostasis under low-Fe stress in *Citrus grandis* (Zhang et al. 2020) have been found in QTL regions I, III and V. Two of them, bHLH 137.1 and ILR3 are predicted to interact with PYE, another bHLH factor that is a key regulator of Fe deficiency responses. In *Arabidopsis*, ILR3 is likely a mobile protein that affects rhizosphere acidification under Fe deficiency and modulates multiple stress responses, including cyst nematode infection (Samira et al. 2018).

A particularly important *Citrus-Poncirus* genomic region corresponds to QTL cluster IV (Figure 6). It includes QTLs for fruit yield (FN and TFW) under both Fe treatments. Noteworthy, response to brassinosteroid stimulus is a biological process that has been associated with yield (Bargsten et al. 2014), and two genes coding for UDP-glucosyl transferase 73C [EC:2.4.1.-] Glc-brassinosteroid (UGT73C) that could inactivate brassinosteroids (Husar et al. 2011) are within this region. A known transcriptional factor, the Ethylene Responsive factor ERF SHN/WIN 1 (Ciclev10027305 in Online Resource 6), that has been suggested as an important candidate for improvement of abiotic stress tolerance in crops (Djemal et al. 2018), is in this region too. It is important to point out that cluster IV region also contains the major QTL governing Citrus Tristeza Virus multiplication (Asins et al. 2012), and two QTLs

for foliar Huanglongbing symptoms (FS-2015-S7a and FS-2016-S7a, Huang et al. 2018). Reductions in Fe and Zn leaf concentrations have been observed after infection by *Candidatus liberribacter* asiaticus, the causal organism of Huanglongbing in Asia (Masaoka et al. 2011). This genomic region is enriched in genes related to DNA metabolic process and cellular response to stress (Online Resource 5), and it is rich in disease resistance genes (Online Resource 6). Noteworthy, cluster II is enriched in genes coding for the regulatory protein NPR1 that is a key regulator of the SA-mediated SAR pathway that mediates cross-talk between salicylic acid and jasmonic/ethylene responses (Backer et al. 2019), and regulates SA-mediated expression of the metal transporter YSL3 (Chen et al. 2014). Cluster II is also rich in AIG1 domain-containing proteins. This domain is related to resistance against bacteria (https://pfam.xfam.org/family/AIG1). Differential proteins related to the plant defense were previously reported when comparing root protein profiles of two citrus rootstocks (low-Fe tolerant and sensitive) under Fe deficiency conditions (Muccilli et al. 2013).

In conclusion, for first time, a genetic analysis of citrus rootstock-mediated tolerance to iron deficiency and total iron fruit content has been carried out unveiling four genomic regions involved in natural genetic variation for those traits, likely harboring candidate genes that deserve future research to assess their final degree of responsibility in explaining total variability in order to be used in molecular breeding programs of citrus rootstocks. A genetic connection between citrus rootstock-mediated tolerance to Fe deficiency and biotic stresses, based on genes within QTL regions II, IV and V, has been found.

Acknowledgments

We thank Mrs. Miryam Rojas at Servicio de Instrumentación Científica de la Estación Experimental del Zaidín (CSIC) for mineral analysis and Mr. José Cerdá for technical assistance. This work was supported by grants from the Spanish Government (MJA) (AGL2014-56675-R, AGL2017-82452-C2-2-R),

Data archiving statement

The SSR primer sequences are available upon request, for scientific purposes only, from the corresponding author mjasins@ivia.es. The genetic linkage maps were submitted to the Citrus Genome Database (https://www.citrusgenomedb.org/). Other markers are described in Raga et al. (2016). The parents of the progeny are kept at the Citrus Germplasm Bank, and the accession references are: IVIA-385 (Cleopatra mandarin), IVIA-537 (Flying Dragon trifoliate orange) and IVIA-236 (Rich trifoliate

orange). Genomic data on candidate genes are provided as electronic supplementary material EMS_6.

Conflict of interest: The authors declare that they have no conflict of interest.

Ethical standards: The authors declare that the experiment complies with the current laws.

References

Abadía J, Alvarez-Fernandez A, Rombolà AD, Sanz M, Tagliavini M, Abadía M (2004) Technologies for the diagnosis and remediation of Fe deficiency. Soil Sci Plant Nutr 50:965-971

Almaliotis DD, Manganaris AG, Simonis AD, Bladenopoulou SB (1995) Rootstock effect on yield and mineral nutrition of 'Maycrest? Peach trees under conditions of lime-induced chlorosis. In: Abadía J (Ed.) Iron nutrition in soils and plants. Kluwer Academic Publishers, Dordrecht, pp 301-306

Asins MJ, Fernández-Ribacoba J, Bernet GP, Gadea J, Cambra M , Gorris MT, Carbonell EA (2012) The position of the major QTL for Citrus tristeza virus resistance is conserved among *Citrus grandis, C. aurantium* and *Poncirus trifoliata*. Molecular Breeding 29:575–587

Asins MJ, Raga MV, Torrent D, Roca D, Carbonell EA (2020) QTL and candidate gene analyses of rootstock-mediated tomato fruit yield and quality traits under low iron stress. Euphytica. https://doi.org/10.1007/s10681-020-02599-6

Backer R, Sanushka Naidoo S, van den Berg N (2019) The NONEXPRESSOR OF PATHOGENESIS-RELATED GENES 1 (NPR1) and related family: mechanistic insights in plant disease resistance. Front Plant Sci 10:102. https://doi.org/10.3389/fpls.2019.00102

Bargsten JW, Nap J-P, Sanchez-Perez GF, van Dijk ADJ (2014) Priorization of candidate genes in QTL regions based on associations between traits and biological processes. BMC Plant Biol 14:330

Barros e Silva AE, Marques A, dos Santos KGB, Guerra M (2010) The evolution of CMA bands in *Citrus* and related genera. Chromosome Res 18:503-5014

Ben Yahmed J, Costantino G, Amiel P, Talon M, Ollitrault P, Morillon R, Luro F (2016) Diversity in the trifoliate orange taxon reveals two main genetic groups marked by specific morphological traits and water deficit tolerance properties. J Agric Sci 154:495-514. https://doi.org/10.1017/S0021859615000234

505 Castle W S, Rom RC, Carlson RF (1987) Rootstocks for fruit crops. Citrus rootstocks.
506 Wiley, New York, p. 361-399
507 Castle WS, Nunnallee J, Manthey JA (2009.) Screening Citrus Rootstocks and Related
508 Selections in Soil and Solution Culture for Tolerance to Low-iron Stress.
509 Hortscience 44: 638-645
510 Chen C-C, Chien W-F, Lin N-C, Yeh K-C (2014) Alternative functions of Arabidopsis
511 YELLOW STRIPE-LIKE3: from metal translocation to pathogen defense. PLOS
512 ONE 9: e98008. https://doi.org/10.1371/journal.pone.0098008
513 Chu H-H, Chiecko J, Punshon T, Lanzirotti A, Lahner B, Salt DE, Walker EL (2010)
514 Successful Reproduction Requires the Function of Arabidopsis YELLOW
515 STRIPE-LIKE1 and YELLOW STRIPE-LIKE3 metal-nicotianamine transporters
516 in both vegetative and reproductive structures. Plant Physiol 154:197–210
517 Czech A, Zarycka E, Yanovych D, Zasadna Z, Grzegorczyk I, Klys S, (2020) Mineral
518 content of the pulp and peel of various citrus fruit cultivars. Biol Trace Elem Res
519 193:555-563. https://doi.org/10.1007/s12011-019-01727-1
520 Djemal R, Mila I, Bouzayen M, Pirrello J, Khoudi H (2018) Molecular cloning and
521 characterization of novel WIN1/SHN1 ethylene responsive transcription factor
522 HvSHN1 in barley (*Hordeum vulgare* L.). J Plant Physiol 228:39-46. https://doi:
523 10.1016/j.jplph.2018.04.019.
524 Fang, D. Q., Roose, M. L., Krueger, R. R. & Federici, C. T. (1997). Fingerprinting
525 trifoliate orange germ plasm accessions with isozymes, RFLPs, and inter-simple
526 sequence repeat markers. Theor Appl Genet 95:211–219.
527 Fernandez V, Winkelmann G, Ebert G (2004) Iron supply to tobacco plants though
528 foliar application of iron citrate and ferric dimerum acid. Physiol Plant 122:380-
529 385
530 Forner-Giner MA, Llosa MJ, Carrasco JL, Perez-Amador MA, Navarro L, Ancillo G
531 (2009) Differential gene expression analysis provides new insights into the
532 molecular basis of iron deficiency stress response in the citrus rootstock *Poncirus*
533 *trifoliata* (L.) Raf. J Exp Bot 61:483-490. https://doi.org/10.1093/jxb/erp328
534 Fu LN, Zhu QQ, Sun YY, Du W, Pan ZY, Peng SA (2017) Physiological and
535 Transcriptional Changes of Three Citrus Rootstock Seedlings under Iron
536 Deficiency. Front Plant Sci 8: 1104. https://doi.org/10.3389/fpls.2017.01104

537 Grattapaglia D, Sederoff RR (1994) Genetic linkage maps of *Eucaliptus grandis* and *E.*
538 *urophylla* using a pseudo-testcross mapping strategy and RAPD markers. Genetics
539 137:1121-1137
540 Herrero R, Asins MJ, Carbonell EA, Navarro L (1996) Genetic diversity in the orange
541 subfamily Aurantioideae. II. Genetic relationships among genera and species.
542 Theor Appl Genet 93:1327-1334
543 Hong YS, Choi JY, Nho EY, Hwang IM, Khan N, Jamila N, Kim KS (2019)
544 Determination of macro, micro and trace elements in citrus fruits by inductively
545 coupled plasma-optical emission spectrometry (ICP-OES), ICP-mass spectrometry
546 and direct mercury analyzer J. Sci. Food Agric 99:1870-1879.
547 https://doi.org/10.1002/jsfa.9382
548 Huang H, Ullah F, Zhou D-X, Yi M, Zhao Y (2019) Mechanisms of ROS regulation of
549 plant development and stress responses. Front Plant Sci 10:800.
550 https://doi.org/10.3389/fpls.2019.00800
551 Huang M, Roose ML, Yu Q, Du D, Yu Y, Zhang Y, Deng Z, Stover E, Gmitter FG
552 (2018) Construction of high-density genetic mapas and detection of QTLs
553 associated with Huanglongbing tolerance in citrus. Front Plant Sci 9:1694
554 https://doi.org/10.3389/fpls.2018.01694
555 Husar S, Berthiller F, Fujioka S, Rozhon W, Khan M, Kalaivanan F, Elias L, Higgins
556 GS, Li Y, Schuhmacher R, Krska R, Seto H, Vaistij FE, Bowles D, Poppenberger
557 B. (2011) Overexpression of the UGT73C6 alters brassinosteroid glucoside
558 formation in *Arabidopsis thaliana*. BMC Plant Biol 11:51.
559 https://doi.org/10.1186/1471-2229-11-51.
560 Jaegger B, Goldbach H, Sommer K (2000) Release from lime induced iron chlorosis by
561 CULTAN in fruit trees and its characterization by analysis Acta Hort 531:107-113
562 Jessop RS, Roth G, Sale P (1990) Effects of increased levels of soil $CaCO_3$ on lupin
563 (*Lupinus angustifolius*) growth and nodulation. Aust J Soil Res 28:955-962
564 Jiao W-B, Huang D, Xing F, Hu Y, Deng X-X, Xu Q, Chen L-L (2013) Genome-wide
565 characterization and expression analysis of genetic variants in sweet orange. The
566 Plant Journal 75:954–964
567 Korcak R (1987) Iron deficiency chlorosis. Hort Rev (Amer Soc Hort Sci) 9:133-186
568 Lado J, Cuellar F, Rodrigo MJ, Zacarias L (2016) Nutritional Composition of
569 Mandarins. In: Simmonds MSJ, Preedy VR (eds) Nutritional composition of fruit

570 cultivars Elsevier Inc pp: 419-443. https://doi.org/10.1016/B978-0-12-408117-
571 8.00018-0
572 Licciardello C, Torrisi B, Allegra M, Sciacca F, Roccuzzo G, Intrigliolo F, Recupero
573 GR, Tononi P, Delledonne M, Muccilli V (2013) A Transcriptomic Analysis of
574 Sensitive and Tolerant Citrus Rootstocks under Natural Iron Deficiency
575 Conditions. J Am Soc Hortic Sci 138: 487-498
576 Lima RPM, Curtolo M, Merfa MV, Cristofani-Yali M, Machado MA (2018) QTLs and
577 eQTLs mapping related to citrandarins resistance to citrus gummosis disease.
578 BMC Genomics 19:516 https://doi.org/10.1186/s12864-018-4888-2
579 Manthey JA, McCoy DL, Crowley DE (1994) Stimulation of rhizosphere iron reduction
580 and uptake in response to iron deficiency in citrus rootstocks. Plant Physiol
581 Biochem 32:211-215
582 Martinez-Cuenca MR, Iglesias DJ, Talon M, Abadia J, Lopez-Millan AF, Primo-Millo
583 E, Legaz F (2013) Metabolic responses to iron deficiency in roots of Carrizo
584 citrange [Citrus sinensis (L.) Osbeck. x Poncirus trifoliata (L.) Raf.] Tree Physiol
585 33:320-329. https://doi.org/10.1093/treephys/tpt011
586 Masaoka Y, Pustika A, Subandiyah S, Okada A, Hanundin E, Purwanto B, Okuda M,
587 Okada Y, Saito A, Holford P, Beattie A, Iwanami T (2011) Lower concentrations
588 of microelements in leaves of citrus infected with *Candidatus Liberibacter*
589 asiaticus. Jarq-Jpn Agr Res Q 45:269-275. https://doi.org/10.6090/jarq.45.269
590 Mendes S, Moraes AP, Mirkov TE, Pedrosa-Harand A (2011) Chromosome
591 homeologies and high variation in heterochromatin distribution between *Citrus* L.
592 and *Poncirus* Raf. as evidenced by comparative cytogenetic mapping.
593 Chromosome Res 19: 521-530 HTTPS://DOI.ORG/10.1007/s10577-011-9203-x
594 Mengel K (1994) Iron availability in plant-tissues-iron chlorosis on calcareous soils.
595 Plant Soil 165: 275-283
596 Muccilli V, Licciardello C, Fontanini D, Cunsolo V, Capocchi A, Saletti R, Torrisi B,
597 Foti S (2013) Root protein profiles of two citrus rootstocks grown under iron
598 sufficiency/deficiency conditions. Eur J Mass Spectrom 19:305-324.
599 https://doi.org/10.1255/ejms.1230
600 Pestana M, de Varennes A, Abadia J, Faria EA (2005) Differential tolerance to iron
601 deficiency of citrus rootstocks grown in nutrient solution. Scientia Horticulturae
602 104: 25-36 HTTPS://DOI.ORG/10.1016/j.scienta.2004.07.007

603 Pestana M, Correia PJ, David M, Abadia A, Abadia J, de Varennes, A (2011) Response
604 of five citrus rootstocks to iron deficiency. J Soil Sci Plant Nutr 174:837-846.
605 https://doi.org/10.1002/jpln.201000341
606 Raga V, Bernet GP, Carbonell EA, Asins MJ (2012) Segregation and linkage analyses
607 in two complex populations derived from the citrus rootstock Cleopatra mandarin.
608 Inheritance of seed reproductive traits. Tree Genetics and Genomes 8:1061-1071
609 Raga V**,** Intrigliolo DS, Bernet GP, Carbonell EA and MJ Asíns. 2016**.** Genetic analysis
610 of salt tolerance in a progeny derived from the citrus rootstocks Cleopatra
611 mandarin and trifoliate orange. Tree Genetics and Genomes 12:34.
612 https://doi.org/10.1007/s11295-016-0991-1
613 Ramos J, Clemente MR, Naya L, Loscos J, Perez-Rontome C, Sato S, Tabata S, Becana
614 M (2007) Phytochelatin synthases of the model legume *Lotus japonicus*. A small
615 multigene family with differential response to cadmium and alternatively spliced
616 variants. Plant Physiol 143:1110-1118
617 Rashid A, Ryan J (2004) Micronutrient constraints to crop production in soils with
618 Mediterranean-type characteristics: A review. J Plant Nutr 27:959-975
619 Ruiz C, Bretó MP, Asins MJ (2000) An efficient methodology to identify sexual
620 seedlings in citrus breeding programs using SSR markers. Euphytica 112:89-94.
621 Samira R, Li B, Kliebenstein D, Li C, Davis E, Gillikin JW, Long TA(2018) The bHLH
622 transcription factor ILR3 modulates multiple stress responses in *Arabidopsis*. Plant
623 Molecular Biology (2018) 97:297–309. https://doi.org/10.1007/s11103-018-0735-
624 8
625 Tian T, Liu Y, Yan H, You Q, Yi X, Du Z, Xu W, Su Z (2017) agriGO v2.0: a GO
626 analysis toolkit for the agricultural community, update. Nucleic Acids Res
627 45:W122-W129. https://doi.org/10.1093/nar/gkx382
628 Van Ooijen JW (2009) MapQTL 6 software for the mapping of quantitative trait loci in
629 experimental populations of diploid species. Kyazma, Wageningen, The
630 Netherlands
631 Van Ooijen JW (2012) JoinMap 4.1 software for the calculation of genetic linkage maps
632 in experimental populations. Kyazma, Wageningen, The Netherlands
633 Varshney RK, Terauchi R, McCouch SR (2014) Harvesting the promising fruits of
634 genomics: applying genome sequencing technologies to crop breeding. PLoS Biol
635 12:e1001883

636 Villalta I, Bernet GP, Carbonell EA, Asins MJ (2007) Comparative QTL analysis of
637 salinity tolerance in terms of fruit yield using two *Solanum* populations of F_7 lines.
638 Theor Appl Genet 114:1001-1017
639 Waters BM, Chu HH, Didonato RJ, Roberts LA, Eisley RB, Lahner B, Salt DE, Walker
640 EL (2006) Mutations in Arabidopsis Yellow Stripe-Like1 and Yellow Stripe-Like3
641 reveal their roles in metal ion homeostasis and loading of metal ions in seeds. Plant
642 Physiol 141: 1446–1458
643 Yang HY, Dong T, Li JF, Wang MY (2016) Molecular cloning, expression, and
644 subcellular localization of a PAL gene from *Citrus reticulata* under iron
645 deficiency. Biol Plantarum 60:482-488. https://doi.org/10.1007/s10535-016-0625-
646 3
647 Zhang X-Y, Qiu J-Y, Hui Q-L, Xu Y-Y, He Y-Z, Peng L-Z, Fu X-Z (2020) Systematic
648 analysis of the basic/helix-loop-helix (bHLH) transcription factor family in
649 pummelo (*Citrus grandis*) and identification of the key members involved in the
650 response to iron deficiency. BMC genomics 21(1): 233.
651 https://doi.org/10.1186/s12864-020-6644-7
652 Wu, G., Terol, J., Ibanez, V. et al. (2018) Genomics of the origin and evolution of
653 Citrus. Nature 554, 311–316. https://doi.org/10.1038/nature25447

654 **Table 1**- The mean (and standard error) of the phenotypic values for the analyzed traits in parents (Cleopatra, Cleo, and Flying Dragon, Pon) and minimum (Min) and
655 maximum (Max) adjusted means in the grafted rootstock-segregating population. The estimated broad sense heritabilities under sufficient (H^2_C) and low-Fe fertilization
656 (H^2_Fe) are also included. Not analysed is denoted by na.

Abbrev.	TRAIT	Cleo_C	Pon_C	Cleo_Fe	Pon_Fe	min_C	max_C	min_Fe	max_Fe	H2_C	H2_Fe
Al_F	[Al] in fruit	1.77±0.27	1.53±0.01	6.96±4.9	2.46±0.18	1.33	12.91	1.39	15.60	0.0000	0.0000
Ca_F	[Ca] in fruit	3116.64±74.75	2621.54±51.81	4978.22±912.02	2609.89±462.22	1531.75	5371.76	1357.26	4814.08	0.0109	0.0000
Cu_F	[Cu] in fruit	6.36±0.31	6.87±1.02	4.27±0.53	5.54±0.75	3.15	8.51	3.52	8.98	0.0031	0.2427
Fe_F	[Fe] in fruit	25.15±1.46	20.42±2.05	18.88±0.89	22.94±2.27	19.32	45.32	14.35	31.55	0.0333	0.0000
K_F	[K] in fruit	16231.33±12.12	14135.5±612.26	14592.02±958.53	15350.2±964.58	9466.87	17660.35	9715.66	17705.60	0.0064	0.4726
Mg_F	[Mg] in fruit	1261.8±4.57	942.91±59.69	1157.95±93.11	1035.36±9	823.92	1276.85	817.77	1409.93	0.2316	0.2659
Mn_F	[Mn] in fruit	10.12±1.63	6.47±1.58	4.57±0.26	5.85±0.81	5.72	18.18	4.36	13.46	0.2115	0.0000
Na_F	[Na] in fruit	88.3±21.56	91.6±47.24	336.46±36.54	74.68±0.19	-90.05	395.26	-15.79	734.16	0.0000	0.0738
P_F	[P] in fruit	3561.01±34.49	3202.36±156.58	3250.25±241.98	3527.71±26.38	1978.95	3881.67	2175.17	4163.97	0.0000	0.1938
S_F	[S] in fruit	1955.32±58.89	1642.13±13.48	1947.28±166.25	1687.36±33.56	1238.23	1940.98	1278.30	2281.79	0.1192	0.1419
Si_F	[Si] in fruit	18.12±0.08	14.6±2.5	20.14±5.04	19.32±0.64	-0.74	22.29	-0.23	21.67	0.3570	0.4561
Zn_F	[Zn] in fruit	30.51±0.58	33.4±2.12	44.11±19.47	32.02±7.51	9.83	64.23	10.28	47.91	0.0000	0.0000
Al_Lf	[Al] in leaf	94.94±6.05	64.91±21.81	119.38±5.19	97.79±37.7	20.48	123.31	23.95	156.40	0.5373	0.4002
Ca_Lf	[Ca] in leaf	27681.79±1155.79	24683.06±3735.64	32006.35±3366.7	26555.95±3743.97	14265.46	37868.72	16937.11	49136.17	0.2504	0.2050
Cu_Lf	[Cu] in leaf	11.55±3.12	8.95±2.7	6.32±2.11	16.11±13.06	2.82	29.66	4.19	34.31	0.0315	0.0000
Fe_Lf	[Fe] in leaf	50.76±3.37	64.5±9.42	52.05±7.12	68.49±0.15	37.69	76.13	36.61	80.83	0.0157	0.2205
K_Lf	[K] in leaf	15122±534.81	18161.53±1202.05	16223.77±1354.4	16237.09±1034.79	13600.02	21174.90	11337.82	21488.85	0.0000	0.0000
Mg_Lf	[Mg] in leaf	1421.42±289.88	1362.5±152.43	2716.25±232.23	1338.99±459.64	970.84	3167.60	932.14	3376.77	0.1869	0.1786
Mn_Lf	[Mn] in leaf	57.52±5.34	25.65±1.57	18.44±0.3	32±6.67	18.46	65.92	13.60	63.00	0.2324	0.1181
Na_Lf	[Na] in leaf	589.12±24.02	362.43±165.8	610.11±85.22	257.02±53.11	151.32	1427.97	192.53	1988.62	0.0239	0.2484
P_Lf	[P] in leaf	2080.33±492	2545.97±451.34	1862.71±69.85	2126.01±2.99	1319.72	3106.53	1046.06	3690.31	0.0511	0.0000
S_Lf	[S] in leaf	2714.06±132.84	2730.46±35.63	2527.08±284.97	2493.17±131.43	1797.83	3304.76	1717.68	3454.48	0.0442	0.0474

Si_Lf	[Si] in leaf	307.84±61.65	170.7±11.02	354.18±41.38	245.46±63.9	122.87	361.80	146.20	438.60	0.3886	0.0709
Zn_Lf	[Zn] in leaf	36.99±11.53	35.23±6.63	30.84±8.3	24.63±1.25	9.59	60.39	13.93	41.93	0.1048	0.0147
Fe_F_Lf	100 (Fe_F/Fe_Lf)	0.33±0.03	0.24±0.01	0.27±0.02	0.25±0.02	0.25	0.46	0.18	0.40	0.0645	0.0000
Al_F_Lf	100 (Al_F/Al_Lf)	0.02±0.0039	0.03±0.01	0.05±0.03	0.03±0.01	0.02	0.25	0.01	0.28	0.0000	0.0000
LDM	Leaf dry matter	39.9±2.4	37.82±4.49	39.85±3.01	41.88±0.97	35.61	48.76	38.35	46.91	0.0000	0.0000
LFW	Leaf fresh weight	2.1±0.5	2.35±0.25	2.35±0.45	2.15±0.05	1.70	4.00	1.70	3.65	0.1757	0.0000
LDW	Leaf dry weight	0.85±0.25	0.9±0.2	0.95±0.25	0.9±0	0.77	1.88	0.68	1.62	0.1574	0.0000
LWC	Leaf water content	1.52±0.16	1.68±0.32	1.52±0.19	1.39±0.05	1.05	1.91	1.12	1.60	0.0000	0.0000
S3	SPAD at the end	77.75±4.95	69.3±1	49.25±18.85	73.9±1.7	65.22	85.38	61.27	80.78	0.1431	0.1187
LA	Leaf area	19.8±1.9	27.8±1.6	25.85±1.15	18.7±0.4	18.27	31.67	17.52	30.03	0.0647	0.0000
FNm	Fruit number	8.5±0.5	5.5±1.5	12±0	7.5±2.5	0.93	23.41	1.99	20.89	0.0248	0.0843
TFWm	Total fruit weight	0.55±0.01	0.47±0.03	0.66±0.14	0.37±0.13	0.13	1.40	0.08	1.35	0.1787	0.1770
TDFWp	Total pulp dry weight	7.76±0.49	6.31±1.07	6.19±0.54	4.22±0.67	1.24	23.59	3.35	19.40	0.0655	0.1421
FeUEp	Total harvested Fe	0.2±0.02	0.13±0.01	0.12±0.0048	0.1±0.02	0.08	0.45	0.06	0.47	0.1376	0.3973
MgUEp	Total harvested Mg	9.79±0.58	6.02±1.39	7.12±0.05	4.36±0.65	1.57	27.39	4.08	19.97	0.0453	0.1654
PUEp	Total harvested P	27.66±2.01	20.38±4.41	19.99±0.27	14.89±2.46	-1.02	81.90	10.18	57.51	0.0000	0.3082
SUEp	Total harvested Fe	15.21±1.42	10.35±1.67	11.97±0.03	7.09±0.98	2.04	43.72	5.52	33.31	0.0643	0.3623
FW	Fruit weight	57.27±7.13	85.69±14.93	52.84±10.02	49.87±3.31	33.64	143.94	45.58	110.80	0.0000	0.0000
FD	Fruit diameter	49.36±1.21	57.61±3.89	48.5±3.21	47.74±0.54	41.00	66.50	46.50	61.88	0.0000	0.0000
RT	Rind thickness	1.93±0.07	2.64±0.36	1.5±0.07	1.36±0.36	1.29	4.00	1.20	3.29	0.0000	0.0000
JV	Juice volume	24.21±2.93	30.71±2.29	26.57±3.71	22.91±1.51	14.64	51.75	19.61	52.54	0.0000	0.0000
JC	Juice content	43.18±0.03	36.5±3.79	51.51±2.59	46.74±1.26	23.63	56.07	35.59	55.43	0.0732	0.0000
SSC	Soluble-solids content	8.2±0.57	7.65±0.4	8.14±1.31	7.55±0.43	6.63	10.48	6.31	10.83	0.0000	0.0060
NaOH	NaOH volume	7.8±0.04	7.69±0.46	8.26±2.1	7.81±0.53	5.69	13.14	5.94	13.38	0.0000	0.2580
SSC_A	SSC/Acidity ratio	8.32±0.51	7.92±0.03	8.67±3.38	7.64±0.04	5.29	11.18	5.70	9.05	0.1311	0.0000
dAl	change in leaf [Al]	68.86±0.54	48.81±25.85	96.98±1.63	63.64±19.09	28.83	99.76	-57.48	117.96	na	0.2091
dCa	change in leaf [Ca]	10787.41±5157.9	7809.84±3449.66	6360.48±830.38	8451.16±5022.27	-1791.34	14021.09	-13547.02	27496.93	na	0.0880

dCu	change in leaf [Cu]	-63.43±26.07	-42.05±17.96	-41.29±6	-37.28±9.02	-57.88	-7.64	-53.57	0.87	na	0.1788
dFe	change in leaf [Fe]	5.71±1.33	17.23±6.53	18.17±6.52	10.7±0.56	-2.82	19.17	-35.19	40.23	na	0.1336
dK	change in leaf [K]	-925.46±725.38	358.67±2180.94	2878.82±1858.36	355.45±1106.42	-2041.60	11093.08	-2564.16	15736.99	na	0.1181
dMg	change in leaf [Mg]	421.67±245.39	604.29±116.98	1064.78±188.44	450.81±387.82	-530.23	792.56	-1168.86	2273.86	na	0.0692
dMn	change in leaf [Mn]	15.88±0.09	2.26±7.05	-6.9±2.2	-0.66±3.96	-14.53	28.00	-12.64	27.35	na	0.0000
dNa	change in leaf [Na]	-65.78±316.67	-243.79±241.26	92.42±26.44	53.82±14.05	-520.42	25.70	-470.62	1745.23	na	0.2482
dP	change in leaf [P]	-780.79±142.5	274.05±28.75	241.76±230.3	-619.34±439.22	-700.47	1040.59	-671.80	1738.10	na	0.0747
dS	change in leaf [S]	-395.61±540.34	-849.58±6.52	-450.98±764.3	-1037.61±607.5	-1187.59	391.47	-1079.52	1181.71	na	0.0000
dSi	change in leaf [Si]	183.19±36.02	88.53±21.36	98.74±10.13	119.36±40.81	-31.48	148.01	-109.25	266.64	na	0.1581
dZn	change in leaf [Zn]	-0.03±13.44	-13.84±10.81	-8.15±0.95	3.26±3.15	-4.66	20.86	-23.67	25.72	na	0.0000

Table 2- List of the position (in cM), LOD, and nearest marker (Locus) to QTLs detected by IM and MQM in the integrated *Citrus reshni-Poncirus trifoliata* genetic linkage map (LG) using the cross-pollinated model. Those QTL that were also detected at the individual parental linkage maps are indicated by adding the parental linkage group between parenthesis (R or Pr for *C. reshni* and *P. trifoliata*, respectively). The four genotypic means (**ac**, **ad, bc**, and **bd**, being *C. reshni* **ab** and *P. trifoliata* **cd**), the percentage of explained variance, PEV, and the genomic region containing QTLs for target traits (Region) are included. These regions, named in Latin numbers (from I to V), were anchored to the *C. clementina* physical map, and the corresponding scaffold number is indicated between parentheses.

Region	Trait	Group	Position	Locus	LOD	ac	ad	bc	bd	PEV
	C_Ca_Lf	4c (R)	0.0	15R,750	3.1	20032.60	27005.10	27607.90	28230.50	20.6
	C_Fe_F	7 (Pr)	104.3	C11iC1rt,400	6.6	24.99	27.97	24.34	34.24	38.9
IV (7)	C_FNm	4b	104.8	Py65C,506	3.7	8.59	16.09	13.84	2.95	24.1
	C_K_F	4c	0.0	15R,750	2.5	13749.50	13721.30	12261.60	14357.20	16.8
	C_Mg_F	3a	20.0	CR31,100	2.8	1220.37	998.07	1033.27	1112.23	18.9
	C_Si_Lf	7	228.8	CAC23,230	3.3	186.04	308.56	215.12	222.71	21.4
	C_SSC/A	3b (R)	8.9	C8iC1rt,650	2.5	7.53	7.08	8.30	7.92	16.9
	C_SSC/A	4b (Pr)	54.4	CR3,320	3.7	8.83	7.42	7.90	6.91	24.4
	C_SUEp	2	64.0	TAA1,180	3.0	76.50	-16.64	-27.37	33.32	20.4
IV (7)	C_TFWm	4b	104.8	Py65C,506	3.8	0.64	1.01	0.85	0.27	24.6
I (3)	Fe_Cu_F	7	71.4	CR17,300	4.9	6.79	5.51	5.37	6.67	29.4
	Fe_Cu_F	3b	9.9	C8iC1rt,650	3.2	6.79	7.34	6.40	5.24	18.3
	Fe_dAl	8 (Pr)	214.7	HD-ZIP,510	3.0	21.34	20.49	47.09	-18.36	20.1
V (1)	Fe_dCu	3b	0.0	C1,1600	2.4	-27.74	-39.33	-38.16	-17.42	16.5
V (1)	Fe_dK	3b	0.0	C1,1600	4.7	1889.38	2115.62	1921.90	8871.46	29.2
II (3)	Fe_FeUEp	7 (Pr)	138.2	C1iC8rt,515	5.2	0.30	0.15	0.19	0.22	31.9
III (4)	Fe_FeUEp	12 (R)	46.8	CMS20,170	3.1	0.21	0.16	0.26	0.24	20.7
III (4)	Fe_FNm	12	41.9	6F5R,1200	3.2	10.19	7.79	14.64	11.48	21.4
IV (7)	Fe_FNm	4b	95.5	Py65C,506	3.2	8.26	13.69	14.21	4.43	21.3
II (3)	Fe_MgUEp	7 (Pr)	137.2	C1iC8rt,515	4.4	13.28	7.19	9.87	9.85	27.6
III (4)	Fe_MgUEp	12 (R)	48.8	CMS20,170	3.9	9.37	7.40	11.92	11.70	24.9
	Fe_Mn_Lf	2	170.1	NAC1,520	3.2	37.59	47.33	41.75	23.84	20.8
	Fe_Na_F	4c (R)	26.8	CR28,270	3.6	197.65	329.86	402.63	363.50	23.4
	Fe_NaOH	12 (R)	172.9	C11iC1rt,350	3.0	5.09	7.71	13.53	10.33	20
II (3)	Fe_PUEp	7 (Pr)	136.2	C1iC8rt,515	4.5	38.42	19.10	27.03	27.36	28.4
III (4)	Fe_PUEp	12 (R)	49.8	CMS20,170	4.1	23.84	20.29	35.38	32.43	26
	Fe_S_F	8 (R8+6)	82.0	EMA_M30	4.7	-1078.06	4705.05	3253.26	-514.32	32
	Fe_S3	10+5b (R)	119.1	CT19,165	3.3	74.39	73.60	72.69	69.26	21.7
V (1)	Fe_S3	3b	0.0	C1,1600	3.6	72.14	75.34	73.56	65.45	23.6

II (3)	Fe_SUEp	7 (Pr)	137.2	C1iC8rt,515	4.8	21.20	10.24	14.59	15.53	29.8
III (4)	Fe_SUEp	12 (R)	48.8	CMS20,170	3.9	14.00	11.07	19.76	17.19	25.2
II (3)	Fe_TDFWp	7	137.2	C1iC8rt,515	4.0	12.31	6.97	9.28	9.62	25.8
III (4)	Fe_TDFWp	12 (R)	44.9	CMS20,170	4.2	8.64	7.28	11.59	10.84	26.6
IV (7)	Fe_TFWm	4b	97.5	Py65C,506	3.3	0.64	0.95	0.93	0.29	21.4

665

Figure Captions

Fig. 1 Schematic representation of the process to obtain the mapping population (discarding nucellar seedlings) from the cross between Cleopatra mandarin and trifoliate orange (at the top). Next step (downwards) was the obtention of nucellar seedlings from 62 apomictic R×Pr hybrids, and 2 parents as controls. Two years after, these seedlings (genetically identical to the mother plant) were grafted with the Clausellina satsuma mandarin (*C. unshiu*). These grafted plants had to grow during 5 years to uniformly yield fruits before establishing the Fe treatments (phenotyped population).

Fig. 2 Distribution of scion traits significantly affected by lowering [Fe] in nutrient solution (Online Resource 2): Fruit [Fe] in ppm (Fe_F), ratio between fruit and leaf Fe concentrations (Fe_F_Lf), leaf SPAD value at the end of experiment (S3), and Leaf [Ca] in ppm (Ca_Lf). Opaque grey indicates trait values under control treatment, and transparent colored, trait values under low-Fe treatment. The parental means are indicated: full black and grey lines for Cleopatra and Flying Dragon in control, respectively, while dashed black and grey lines are the corresponding in low-Fe condition.

Fig. 3 Graphic representation of principal component analysis from the correlation matrix among vegetative, mineral, and fruit yield and quality traits in the grafted *Citrus* x *Poncirus* population under control iron conditions. Most important positive relationships are encircled.

Fig. 4 Graphic representation of principal component analysis from the correlation matrix among vegetative, mineral, and fruit yield and quality traits in the grafted *Citrus* x *Poncirus* population under low-Fe stress. Most important positive relationships are encircled.

Fig. 5 Genotypic means and standard errors for significant epistatic interactions between QTL markers and/or cofactors governing two traits: (A) Cu fruit concentration under low Fe (between Fe_Cu_F QTLs markers CR17,300 and C8iC1rt,650), and (B) leaf SPAD values under low Fe (between Fe_S3 QTLs markers CT19.165 and C1,1600). Genotypes are coded as **ac**, **ad**, **bc** and **bd** (being *C. reshni* **ab** and *P. trifoliata* **cd)**, at the first locus (X axis), and a square (**ll, ac**), a triangle (**lm, ad**), a circle (**bc**) or an asterisk (**bd**) at the second locus.

Fig. 6 LOD profiles of QTLs involved in rootstock mediated tolerance to iron deficiency and fruit quality traits that group together in three genomic regions (regions II to IV in Table 2). Genetic positions (markers) along the three integrated *Citrus*-*Poncirus* linkage groups are shown under the X axis. Selected marker intervals, estimated physical distance, and number of genes downloaded from the *C. clementina* data base at https://phytozome.jgi.doe.gov are included.

Electronic Supplementary Material

ESM_1 *P*-values of significantly ($p<0.05$) different traits between parents (Cleopatra and Flying Dragon) as rootstocks. Non-significant is denoted as ns.

ESM_2 *P*-values for the significant effects in the mixed model analysis.

ESM_3 Pearson coefficients of significantly correlated traits ($p \leq 0.05$) between Fe treatments.

ESM_4 Pearson coefficients between significantly correlated traits ($p \leq 0.02$) under control (left side) and low-Fe conditions (right side).

ESM_5 Overrepresented Biological Processes and Molecular Functions within QTL genomic regions detected for tolerance to low iron stress and related traits using the Singular Enrichment Analysis tool with the Fisher´s Exact with FDR multiple test correction (Tian et al. 2017) at the AgriGo platform (http://systemsbiology.cau.edu.cn/agriGOv2/).

ESM_6 Summary list of candidate genes (transcripts) downloaded from the *C. clementina* genome database at https://phytozome.jgi.doe.gov within the marker intervals for the QTL regions I, II, II, IV and V. The number of observed (Obs) from total (Tot) annotated genes of each type is indicated except when a different annotation was obtained from NCBI (between parenthesis). Only one transcript of each type is provided, as well its start and end physical positions in bp.

Manuscript entitled “QTL and candidate gene analyses of rootstock-mediated mandarin fruit yield and quality traits under contrasting iron availabilities” submitted to TGG by MJ Asins (mjasins@ivia.es), MV Raga, D Roca and EA Carbonell

ESM_1 *P*-values of significantly ($p<0.05$) different traits between parents (Cleopatra and Flying Dragon) as rootstocks. Non-significant is denoted as ns.

Trait	p (Control)	p (Low-Fe)
Ca_F	ns	0.0080
Mg_F	0.0070	ns
Mg_Lf	ns	0.0430
Mn_Lf	0.0060	ns
Si_Lf	0.0100	ns
S3	ns	0.0003
LA	0.0440	ns
dP	0.0160	ns

Manuscript entitled “QTL and candidate gene analyses of rootstock-mediated mandarin fruit yield and quality traits under contrasting iron availabilities” submitted to TGG by MJ Asins (mjasins@ivia.es), MV Raga, D Roca and EA Carbonell

ESM_2 *P*-values for the significant effects in the mixed model analysis.

Abbrev.	TRAIT	G	E	GxE
Al_F	[Al] in fruit			
Ca_F	[Ca] in fruit			
Cu_F	[Cu] in fruit	0.0149		
Fe_F	[Fe] in fruit		0.0183	
K_F	[K] in fruit	0.0087		
Mg_F	[Mg] in fruit	0.0007		
Mn_F	[Mn] in fruit			
Na_F	[Na] in fruit			
P_F	[P] in fruit			
S_F	[S] in fruit	0.0242		
Si_F	[Si] in fruit	<0.0001		
Zn_F	[Zn] in fruit			
Al_Lf	[Al] in leaf	<0.0001		
Ca_Lf	[Ca] in leaf	0.0077		0.0048
Cu_Lf	[Cu] in leaf			
Fe_Lf	[Fe] in leaf	0.0061		
K_Lf	[K] in leaf	0.017		
Mg_Lf	[Mg] in leaf	0.0006		
Mn_Lf	[Mn] in leaf	0.0039		
Na_Lf	[Na] in leaf	0.0085		
P_Lf	[P] in leaf	0.023		
S_Lf	[S] in leaf	0.0296		
Si_Lf	[Si] in leaf	0.0012		
Zn_Lf	[Zn] in leaf	0.0288		
Fe_F_Lf	100 (Fe_F/Fe_Lf)		0.0241	
Al_F_Lf	100 (Al_F/Al_Lf)			
LDM	Leaf dry matter			
LFW	Leaf fresh weight			
LDW	Leaf dry weight			
LWC	Leaf water content			
S3	SPAD at the end	0.0021	0.0062	
LA	Leaf area			
FNm	Fruit number	0.0319		
TFWm	Total fruit weight	0.0007		
TDFWp	Total pulp dry weight	0.0031		
FeUEp	Total harvested Fe	0.0001		
MgUEp	Total harvested Mg	0.0051		
PUEp	Total harvested P	0.0037		

SUEp	Total harvested Fe	<0.0001		
FW	Fruit weight			
FD	Fruit diameter			
RT	Rind thickness			
JV	Juice volume			
JC	Juice content			
SSC	Soluble-solids content			
NaOH	NaOH volume			
SSC_A	SSC/Acidity ratio			

Manuscript entitled "QTL and candidate gene analyses of rootstock-mediated mandarin fruit yield and quality traits under contrasting iron availabilities" submitted to TGG by MJ Asins (mjasins@ivia.es), MV Raga, D Roca and EA Carbonell

ESM_3 Pearson coefficients of significantly correlated traits ($p \leq 0.05$) between Fe treatments.

Trait 1	Trait 2	Pearson	*p*-value
Fe_Al_Lf	C_Al_Lf	0.70	<0.0001
Fe_FNm	C_FNm	0.41	0.0008
Fe_K_Lf	C_K_Lf	0.40	0.0011
Fe_Mg_Lf	C_Mg_Lf	0.37	0.0033
Fe_Mn_Lf	C_Mn_Lf	0.26	0.0392
Fe_P_Lf	C_P_Lf	0.41	0.0008
Fe_PUEp	C_PUEp	0.27	0.0359
Fe_S_Lf	C_S_Lf	0.33	0.0098
Fe_S3	C_S3	0.42	0.0008
Fe_Si_F	C_Si_F	0.61	<0.0001
Fe_Si_Lf	C_Si_Lf	0.27	0.0343
Fe_SSC	C_SSC	0.33	0.0103
Fe_TDFWp	C_TDFWp	0.28	0.0298
Fe_TFWm	C_TFWm	0.46	0.0001

Manuscript entitled "QTL and candidate gene analyses of rootstock-mediated mandarin fruit yield and quality traits under contrasting iron availabilities" submitted to TGG by MJ Asins (mjasins@ivia.es), MV Raga, D Roca and EA Carbonell

ESM_4 Pearson coefficients between significantly correlated traits ($p \leq 0.02$) under control (left side) and low-Fe conditions (right side).

Trait 1	Trait 2	Pearson	p-value
C_Al_F	C_Al_F_Lf	0.74	<0.0001
C_Al_Lf	C_Al_F_Lf	-0.50	<0.0001
C_Al_Lf	C_Fe_F_Lf	-0.39	0.0015
C_Ca_Lf	C_Fe_F_Lf	-0.35	0.0055
C_Cu_F	C_FeUEp	0.38	0.0029
C_Cu_F	C_Mn_Lf	0.50	<0.0001
C_Cu_F	C_PUEp	0.30	0.0173
C_Cu_F	C_SUEp	0.30	0.0181
C_Cu_Lf	C_Fe_F_Lf	-0.31	0.0157
C_Cu_Lf	C_PUEp	0.33	0.0099
C_Cu_Lf	C_SUEp	0.32	0.0107
C_Fe_F	C_Ca_F	0.47	0.0001
C_Fe_F	C_Fe_F_Lf	0.71	<0.0001
C_Fe_F	C_MgUEp	-0.46	0.0002
C_Fe_F	C_Na_Lf	-0.33	0.0094
C_Fe_F	C_PUEp	-0.45	0.0002
C_Fe_F	C_SUEp	-0.39	0.0019
C_Fe_F	C_TDFWp	-0.50	<0.0001
C_Fe_F_Lf	C_MgUEp	-0.35	0.006
C_Fe_F_Lf	C_PUEp	-0.36	0.0049
C_Fe_F_Lf	C_SUEp	-0.30	0.0188
C_Fe_F_Lf	C_TDFWp	-0.38	0.0026
C_Fe_Lf	C_Ca_Lf	0.43	0.0005
C_Fe_Lf	C_Cu_Lf	0.42	0.0007
C_Fe_Lf	C_Fe_F_Lf	-0.31	0.0157
C_FeUEp	C_TDFWp	0.84	<0.0001
C_FNm	C_Cu_Lf	0.33	0.0094
C_FNm	C_Fe_F	-0.32	0.0107
C_FNm	C_Fe_F_Lf	-0.38	0.0021
C_FNm	C_FeUEp	0.57	<0.0001
C_FNm	C_FW	-0.60	<0.0001
C_FNm	C_JC	0.36	0.0042
C_FNm	C_JV	-0.53	<0.0001
C_FNm	C_Mg_Lf	0.42	0.0008
C_FNm	C_MgUEp	0.63	<0.0001
C_FNm	C_NaOH	0.41	0.0012
C_FNm	C_P_F	0.40	0.0011

Trait 1	Trait 2	Pearson	p-value
Fe_Al_F	Fe_Al_F_Lf	0.81	<0.0001
Fe_Al_Lf	Fe_Al_F_Lf	-0.47	0.0001
Fe_Ca_Lf	Fe_Fe_F_Lf	-0.46	0.0002
Fe_Ca_Lf	Fe_LDM	0.39	0.0017
Fe_Cu_F	Fe_Fe_F_Lf	0.39	0.0019
Fe_Cu_F	Fe_FeUEp	0.34	0.0067
Fe_Cu_F	Fe_Mn_Lf	0.30	0.0196
Fe_Cu_F	Fe_PUEp	0.31	0.0146
Fe_Cu_Lf	Fe_Al_Lf	0.36	0.004
Fe_Fe_F	Fe_Ca_F	0.35	0.0051
Fe_Fe_F	Fe_Cu_F	0.52	<0.0001
Fe_Fe_F	Fe_Fe_F_Lf	0.53	<0.0001
Fe_Fe_F	Fe_FeUEp	0.34	0.0062
Fe_Fe_F	Fe_Mn_Lf	0.38	0.0023
Fe_Fe_Lf	Fe_Ca_Lf	0.60	<0.0001
Fe_Fe_Lf	Fe_Cu_Lf	0.37	0.0034
Fe_Fe_Lf	Fe_Fe_F_Lf	-0.67	<0.0001
Fe_Fe_Lf	Fe_LDM	0.34	0.0061
Fe_FeUEp	Fe_TDFWp	0.88	<0.0001
Fe_FNm	Fe_Cu_Lf	0.36	0.0046
Fe_FNm	Fe_FeUEp	0.56	<0.0001
Fe_FNm	Fe_FW	-0.51	<0.0001
Fe_FNm	Fe_JV	-0.55	<0.0001
Fe_FNm	Fe_Mg_Lf	0.48	0.0001
Fe_FNm	Fe_MgUEp	0.64	<0.0001
Fe_FNm	Fe_Mn_Lf	0.34	0.0072
Fe_FNm	Fe_NaOH	0.58	<0.0001
Fe_FNm	Fe_PUEp	0.66	<0.0001
Fe_FNm	Fe_Si_Lf	0.40	0.0015
Fe_FNm	Fe_SSC	0.70	<0.0001
Fe_FNm	Fe_SUEp	0.68	<0.0001
Fe_FNm	Fe_TDFWp	0.72	<0.0001
Fe_FW	Fe_Ca_F	-0.33	0.0086
Fe_FW	Fe_Fe_F_Lf	0.31	0.0128
Fe_FW	Fe_FeUEp	-0.33	0.0078
Fe_FW	Fe_JC	-0.40	0.0014
Fe_FW	Fe_JV	0.88	<0.0001

C_FNm	C_PUEp	0.70	<0.0001
C_FNm	C_Si_Lf	0.40	0.0014
C_FNm	C_SSC	0.54	<0.0001
C_FNm	C_SUEp	0.66	<0.0001
C_FNm	C_TDFWp	0.66	<0.0001
C_FW	C_FeUEp	-0.39	0.0021
C_FW	C_JC	-0.59	<0.0001
C_FW	C_JV	0.80	<0.0001
C_FW	C_K_Lf	0.30	0.0185
C_FW	C_MgUEp	-0.37	0.0036
C_FW	C_NaOH	-0.60	<0.0001
C_FW	C_PUEp	-0.43	0.0006
C_FW	C_RT	0.63	<0.0001
C_FW	C_SSC	-0.60	<0.0001
C_FW	C_SSC_A	0.47	0.0001
C_FW	C_SUEp	-0.41	0.0011
C_FW	C_TDFWp	-0.44	0.0003
C_FW	C_Zn_Lf	-0.41	0.0011
C_JC	C_Ca_F	0.31	0.0144
C_JC	C_FeUEp	0.32	0.0123
C_JC	C_K_F	-0.34	0.0076
C_JC	C_K_Lf	-0.33	0.0103
C_JC	C_NaOH	0.48	0.0001
C_JC	C_SSC	0.34	0.0067
C_JC	C_SSC_A	-0.49	0.0001
C_JV	C_Fe_F	0.33	0.0085
C_JV	C_Fe_F_Lf	0.40	0.0014
C_JV	C_MgUEp	-0.34	0.0079
C_JV	C_Na_F	-0.31	0.0139
C_JV	C_Na_Lf	-0.31	0.0161
C_JV	C_NaOH	-0.39	0.0016
C_JV	C_PUEp	-0.41	0.0009
C_JV	C_SSC	-0.54	<0.0001
C_JV	C_SUEp	-0.37	0.0033
C_JV	C_TDFWp	-0.40	0.0014
C_JV	C_Zn_Lf	-0.39	0.0017
C_K_F	C_Cu_F	0.38	0.0026
C_K_F	C_P_Lf	0.38	0.0022
C_K_F	C_PUEp	0.32	0.0128
C_LA	C_Cu_Lf	-0.31	0.0135
C_LA	C_K_Lf	-0.30	0.0198
C_LDW	C_LDM	0.39	0.0023
C_LFW	C_Al_F_Lf	0.34	0.007
C_LFW	C_LDW	0.96	<0.0001
C_LWC	C_LDM	-0.98	<0.0001
C_LWC	C_LDW	-0.39	0.0022

Fe_FW	Fe_LDM	-0.30	0.0176
Fe_FW	Fe_MgUEp	-0.40	0.0011
Fe_FW	Fe_NaOH	-0.60	<0.0001
Fe_FW	Fe_P_F	-0.37	0.0027
Fe_FW	Fe_PUEp	-0.49	<0.0001
Fe_FW	Fe_RT	0.47	0.0001
Fe_FW	Fe_SSC	-0.45	0.0002
Fe_FW	Fe_SSC_A	0.42	0.0006
Fe_FW	Fe_SUEp	-0.46	0.0002
Fe_FW	Fe_TDFWp	-0.43	0.0006
Fe_JC	Fe_Ca_F	0.39	0.0018
Fe_JV	Fe_FeUEp	-0.37	0.0033
Fe_JV	Fe_Mg_Lf	-0.34	0.0069
Fe_JV	Fe_MgUEp	-0.50	<0.0001
Fe_JV	Fe_NaOH	-0.61	<0.0001
Fe_JV	Fe_P_F	-0.44	0.0004
Fe_JV	Fe_PUEp	-0.59	<0.0001
Fe_JV	Fe_SSC	-0.52	<0.0001
Fe_JV	Fe_SSC_A	0.37	0.003
Fe_JV	Fe_SUEp	-0.53	<0.0001
Fe_JV	Fe_TDFWp	-0.51	<0.0001
Fe_K_F	Fe_Cu_F	0.39	0.0019
Fe_K_F	Fe_MgUEp	0.32	0.0124
Fe_K_F	Fe_PUEp	0.39	0.002
Fe_LDM	Fe_Fe_F_Lf	-0.32	0.0113
Fe_LDW	Fe_LDM	0.59	<0.0001
Fe_LFW	Fe_LDM	0.33	0.0091
Fe_LFW	Fe_LDW	0.95	<0.0001
Fe_LFW	Fe_LWC	-0.35	0.0047
Fe_LWC	Fe_Ca_Lf	-0.39	0.0017
Fe_LWC	Fe_Fe_F_Lf	0.32	0.0109
Fe_LWC	Fe_Fe_Lf	-0.34	0.0067
Fe_LWC	Fe_FNm	-0.30	0.0187
Fe_LWC	Fe_FW	0.32	0.0125
Fe_LWC	Fe_LDM	-0.99	<0.0001
Fe_LWC	Fe_LDW	-0.61	<0.0001
Fe_LWC	Fe_Mg_Lf	-0.33	0.008
Fe_LWC	Fe_S_Lf	-0.33	0.0083
Fe_Mg_Lf	Fe_Ca_Lf	0.39	0.0018
Fe_Mg_Lf	Fe_Fe_F_Lf	-0.42	0.0007
Fe_Mg_Lf	Fe_LDM	0.31	0.0157
Fe_Mg_Lf	Fe_MgUEp	0.33	0.0094
Fe_Mg_Lf	Fe_PUEp	0.38	0.0024
Fe_Mg_Lf	Fe_SUEp	0.34	0.0075
Fe_MgUEp	Fe_FeUEp	0.89	<0.0001
Fe_MgUEp	Fe_TDFWp	0.93	<0.0001

C_LWC	C_Na_F	0.36	0.0041
C_Mg_Lf	C_Ca_Lf	0.48	0.0001
C_Mg_Lf	C_Fe_F_Lf	-0.40	0.0014
C_Mg_Lf	C_MgUEp	0.34	0.008
C_Mg_Lf	C_PUEp	0.31	0.0151
C_MgUEp	C_FeUEp	0.81	<0.0001
C_MgUEp	C_TDFWp	0.96	<0.0001
C_Mn_F	C_Ca_F	0.41	0.001
C_Mn_F	C_Cu_F	0.31	0.015
C_Mn_F	C_Fe_F	0.63	<0.0001
C_Mn_F	C_Fe_F_Lf	0.39	0.0017
C_Mn_F	C_Mn_Lf	0.38	0.002
C_Mn_Lf	C_Fe_Lf	0.48	0.0001
C_Na_F	C_Ca_Lf	0.50	<0.0001
C_Na_F	C_LDM	-0.31	0.0136
C_Na_F	C_Mg_Lf	0.33	0.008
C_Na_F	C_Na_Lf	0.43	0.0004
C_Na_F	C_PUEp	0.31	0.0136
C_Na_F	C_Si_Lf	0.36	0.0043
C_Na_F	C_Zn_Lf	0.35	0.0047
C_Na_Lf	C_Ca_Lf	0.44	0.0004
C_Na_Lf	C_MgUEp	0.35	0.0064
C_Na_Lf	C_PUEp	0.38	0.0024
C_Na_Lf	C_SUEp	0.36	0.0046
C_Na_Lf	C_TDFWp	0.32	0.0125
C_NaOH	C_MgUEp	0.30	0.0191
C_NaOH	C_PUEp	0.35	0.0052
C_NaOH	C_S_Lf	-0.33	0.0099
C_NaOH	C_SSC_A	-0.83	<0.0001
C_NaOH	C_SUEp	0.32	0.0108
C_NaOH	C_TDFWp	0.33	0.0098
C_P_F	C_Ca_Lf	0.30	0.0172
C_P_F	C_Cu_F	0.55	<0.0001
C_P_F	C_K_F	0.73	<0.0001
C_P_F	C_Mg_Lf	0.36	0.0037
C_P_F	C_MgUEp	0.37	0.0033
C_P_F	C_Na_F	0.42	0.0006
C_P_F	C_P_Lf	0.41	0.0008
C_P_F	C_PUEp	0.50	<0.0001
C_P_F	C_Si_Lf	0.39	0.002
C_P_F	C_SUEp	0.45	0.0003
C_P_Lf	C_K_Lf	0.57	<0.0001
C_P_Lf	C_Mg_Lf	0.52	<0.0001
C_P_Lf	C_Mn_Lf	0.35	0.0052
C_PUEp	C_FeUEp	0.81	<0.0001
C_PUEp	C_MgUEp	0.96	<0.0001

Fe_Mn_F	Fe_Ca_F	0.40	0.0013
Fe_Mn_F	Fe_Cu_F	0.51	<0.0001
Fe_Mn_F	Fe_Fe_F	0.53	<0.0001
Fe_Mn_F	Fe_Fe_F_Lf	0.45	0.0002
Fe_Mn_F	Fe_FeUEp	0.37	0.0033
Fe_Mn_F	Fe_Mn_Lf	0.63	<0.0001
Fe_Mn_F	Fe_Na_Lf	-0.36	0.0046
Fe_Mn_Lf	Fe_FeUEp	0.30	0.0192
Fe_Mn_Lf	Fe_K_Lf	0.43	0.0006
Fe_Na_F	Fe_Mn_F	-0.30	0.0176
Fe_Na_F	Fe_Na_Lf	0.50	<0.0001
Fe_Na_Lf	Fe_Ca_Lf	0.35	0.0052
Fe_Na_Lf	Fe_Mg_Lf	0.32	0.0105
Fe_Na_Lf	Fe_Mn_Lf	-0.30	0.0183
Fe_NaOH	Fe_Fe_F_Lf	-0.31	0.0135
Fe_NaOH	Fe_FeUEp	0.35	0.005
Fe_NaOH	Fe_K_F	0.31	0.0139
Fe_NaOH	Fe_Mg_Lf	0.38	0.002
Fe_NaOH	Fe_MgUEp	0.48	0.0001
Fe_NaOH	Fe_P_F	0.42	0.0008
Fe_NaOH	Fe_PUEp	0.59	<0.0001
Fe_NaOH	Fe_S_F	0.35	0.0047
Fe_NaOH	Fe_Si_Lf	0.40	0.0013
Fe_NaOH	Fe_SSC_A	-0.78	<0.0001
Fe_NaOH	Fe_SUEp	0.57	<0.0001
Fe_NaOH	Fe_TDFWp	0.48	0.0001
Fe_P_F	Fe_Cu_F	0.53	<0.0001
Fe_P_F	Fe_K_F	0.80	<0.0001
Fe_P_F	Fe_Mg_Lf	0.39	0.002
Fe_P_F	Fe_MgUEp	0.41	0.001
Fe_P_F	Fe_PUEp	0.55	<0.0001
Fe_P_F	Fe_Si_Lf	0.30	0.0186
Fe_P_F	Fe_SUEp	0.46	0.0002
Fe_P_Lf	Fe_K_Lf	0.74	<0.0001
Fe_P_Lf	Fe_Mg_Lf	0.52	<0.0001
Fe_P_Lf	Fe_Mn_Lf	0.45	0.0003
Fe_PUEp	Fe_FeUEp	0.83	<0.0001
Fe_PUEp	Fe_MgUEp	0.96	<0.0001
Fe_PUEp	Fe_TDFWp	0.90	<0.0001
Fe_RT	Fe_JC	-0.65	<0.0001
Fe_RT	Fe_K_Lf	0.32	0.0108
Fe_RT	Fe_P_Lf	0.34	0.0076
Fe_S_F	Fe_Ca_F	0.46	0.0002
Fe_S_F	Fe_Cu_F	0.53	<0.0001
Fe_S_F	Fe_FeUEp	0.35	0.0047
Fe_S_F	Fe_K_F	0.59	<0.0001

C_PUEp	C_TDFWp	0.95	<0.0001
C_RT	C_JC	-0.72	<0.0001
C_RT	C_NaOH	-0.43	0.0006
C_RT	C_SSC_A	0.56	<0.0001
C_S_F	C_Cu_F	0.50	<0.0001
C_S_F	C_Fe_F	0.32	0.0106
C_S_F	C_K_F	0.59	<0.0001
C_S_F	C_P_F	0.71	<0.0001
C_S_Lf	C_Ca_Lf	0.46	0.0001
C_S_Lf	C_Fe_Lf	0.50	<0.0001
C_S_Lf	C_K_Lf	0.44	0.0003
C_S_Lf	C_Mn_Lf	0.40	0.0012
C_S_Lf	C_P_Lf	0.34	0.0066
C_S_Lf	C_TDFWp	-0.31	0.0156
C_S3	C_Cu_F	0.34	0.0066
C_S3	C_Mg_Lf	-0.32	0.0113
C_Si_F	C_Al_F	0.39	0.002
C_Si_F	C_Al_Lf	0.45	0.0003
C_Si_F	C_K_F	0.40	0.0014
C_Si_F	C_S_F	0.30	0.0179
C_Si_F	C_Zn_Lf	0.33	0.0078
C_Si_Lf	C_Ca_Lf	0.47	0.0001
C_Si_Lf	C_Cu_Lf	0.33	0.0094
C_Si_Lf	C_Fe_F_Lf	-0.47	0.0001
C_Si_Lf	C_Fe_Lf	0.44	0.0004
C_Si_Lf	C_Mg_Lf	0.57	<0.0001
C_Si_Lf	C_Mn_Lf	0.35	0.0055
C_Si_Lf	C_P_Lf	0.53	<0.0001
C_SSC	C_Fe_F_Lf	-0.39	0.0018
C_SSC	C_FeUEp	0.42	0.0008
C_SSC	C_K_Lf	-0.30	0.019
C_SSC	C_MgUEp	0.47	0.0001
C_SSC	C_NaOH	0.62	<0.0001
C_SSC	C_PUEp	0.49	0.0001
C_SSC	C_S_Lf	-0.32	0.0119
C_SSC	C_SUEp	0.48	0.0001
C_SSC	C_TDFWp	0.52	<0.0001
C_SUEp	C_FeUEp	0.84	<0.0001
C_SUEp	C_MgUEp	0.96	<0.0001
C_SUEp	C_PUEp	0.98	<0.0001
C_SUEp	C_TDFWp	0.94	<0.0001
C_TFWm	C_FeUEp	0.60	<0.0001
C_TFWm	C_FNm	0.85	<0.0001
C_TFWm	C_FW	-0.32	0.011
C_TFWm	C_Mg_Lf	0.33	0.0085
C_TFWm	C_MgUEp	0.59	<0.0001

Fe_S_F	Fe_MgUEp	0.39	0.0019
Fe_S_F	Fe_P_F	0.80	<0.0001
Fe_S_F	Fe_PUEp	0.51	<0.0001
Fe_S_F	Fe_SUEp	0.56	<0.0001
Fe_S_Lf	Fe_Ca_Lf	0.52	<0.0001
Fe_S_Lf	Fe_Fe_F_Lf	-0.46	0.0002
Fe_S_Lf	Fe_Fe_Lf	0.59	<0.0001
Fe_S_Lf	Fe_K_Lf	0.42	0.0007
Fe_S_Lf	Fe_LDM	0.35	0.0059
Fe_S_Lf	Fe_Mn_Lf	0.43	0.0005
Fe_S_Lf	Fe_P_Lf	0.35	0.0053
Fe_S3	Fe_Fe_F	0.40	0.0014
Fe_S3	Fe_JV	-0.30	0.0169
Fe_Si_F	Fe_Al_Lf	0.61	<0.0001
Fe_Si_F	Fe_Ca_F	0.41	0.0008
Fe_Si_F	Fe_K_F	0.32	0.0109
Fe_Si_F	Fe_Na_F	-0.35	0.0052
Fe_Si_F	Fe_P_F	0.37	0.003
Fe_Si_F	Fe_S_F	0.46	0.0002
Fe_Si_F	Fe_Zn_LF	0.31	0.0146
Fe_Si_Lf	Fe_Ca_Lf	0.52	<0.0001
Fe_Si_Lf	Fe_Cu_Lf	0.45	0.0003
Fe_Si_Lf	Fe_Fe_F_Lf	-0.56	<0.0001
Fe_Si_Lf	Fe_Fe_Lf	0.53	<0.0001
Fe_Si_Lf	Fe_Mg_Lf	0.64	<0.0001
Fe_Si_Lf	Fe_Na_Lf	0.48	0.0001
Fe_Si_Lf	Fe_P_Lf	0.34	0.0071
Fe_Si_Lf	Fe_PUEp	0.32	0.0111
Fe_Si_Lf	Fe_SUEp	0.30	0.0169
Fe_SSC	Fe_Cu_Lf	0.30	0.0176
Fe_SSC	Fe_Fe_F_Lf	-0.30	0.0173
Fe_SSC	Fe_K_Lf	0.30	0.0165
Fe_SSC	Fe_Mg_Lf	0.37	0.0032
Fe_SSC	Fe_MgUEp	0.38	0.0025
Fe_SSC	Fe_NaOH	0.72	<0.0001
Fe_SSC	Fe_P_Lf	0.32	0.012
Fe_SSC	Fe_PUEp	0.48	0.0001
Fe_SSC	Fe_Si_Lf	0.41	0.0009
Fe_SSC	Fe_SUEp	0.51	<0.0001
Fe_SSC	Fe_TDFWp	0.55	<0.0001
Fe_SSC_A	Fe_K_F	-0.45	0.0002
Fe_SSC_A	Fe_MgUEp	-0.31	0.0153
Fe_SSC_A	Fe_P_F	-0.49	<0.0001
Fe_SSC_A	Fe_PUEp	-0.36	0.004
Fe_SSC_A	Fe_S_F	-0.39	0.0018
Fe_SSC_A	Fe_SUEp	-0.32	0.0123

C_TFWm	C_Mn_Lf	0.31	0.014
C_TFWm	C_PUEp	0.62	<0.0001
C_TFWm	C_Si_Lf	0.31	0.0143
C_TFWm	C_SSC	0.36	0.0042
C_TFWm	C_SUEp	0.59	<0.0001
C_TFWm	C_TDFWp	0.62	<0.0001
C_Zn_F	C_Al_F	0.39	0.0018
C_Zn_F	C_Na_F	0.31	0.0158
C_Zn_F	C_P_F	0.39	0.0016
C_Zn_F	C_S_F	0.35	0.0052
C_Zn_F	C_Si_F	0.30	0.0166
C_Zn_Lf	C_Al_Lf	0.40	0.0013
C_Zn_Lf	C_Ca_Lf	0.37	0.0032

Fe_SUEp	Fe_FeUEp	0.87	<0.0001
Fe_SUEp	Fe_MgUEp	0.94	<0.0001
Fe_SUEp	Fe_PUEp	0.97	<0.0001
Fe_SUEp	Fe_TDFWp	0.91	<0.0001
Fe_TFWm	Fe_FeUEp	0.44	0.0004
Fe_TFWm	Fe_FNm	0.84	<0.0001
Fe_TFWm	Fe_K_Lf	0.34	0.0071
Fe_TFWm	Fe_Mg_Lf	0.41	0.0008
Fe_TFWm	Fe_MgUEp	0.47	0.0001
Fe_TFWm	Fe_Mn_Lf	0.43	0.0004
Fe_TFWm	Fe_P_Lf	0.33	0.0085
Fe_TFWm	Fe_PUEp	0.47	0.0001
Fe_TFWm	Fe_SSC	0.55	<0.0001
Fe_TFWm	Fe_SUEp	0.50	<0.0001
Fe_TFWm	Fe_TDFWp	0.57	<0.0001
Fe_Zn_F	Fe_Al_F_Lf	0.32	0.0102
Fe_Zn_F	Fe_Ca_Lf	-0.30	0.0167
Fe_Zn_F	Fe_Si_Lf	-0.30	0.018
Fe_Zn_LF	Fe_Al_Lf	0.38	0.0023
Fe_Zn_LF	Fe_Ca_Lf	0.46	0.0001
Fe_Zn_LF	Fe_Fe_F_Lf	-0.36	0.0044
Fe_Zn_LF	Fe_Fe_Lf	0.36	0.0045
Fe_Zn_LF	Fe_Si_Lf	0.36	0.0044

ESM_5 Overrepresented Biological Processes and Molecular Functions within QTL genomic regions.

Biological Process in Region II

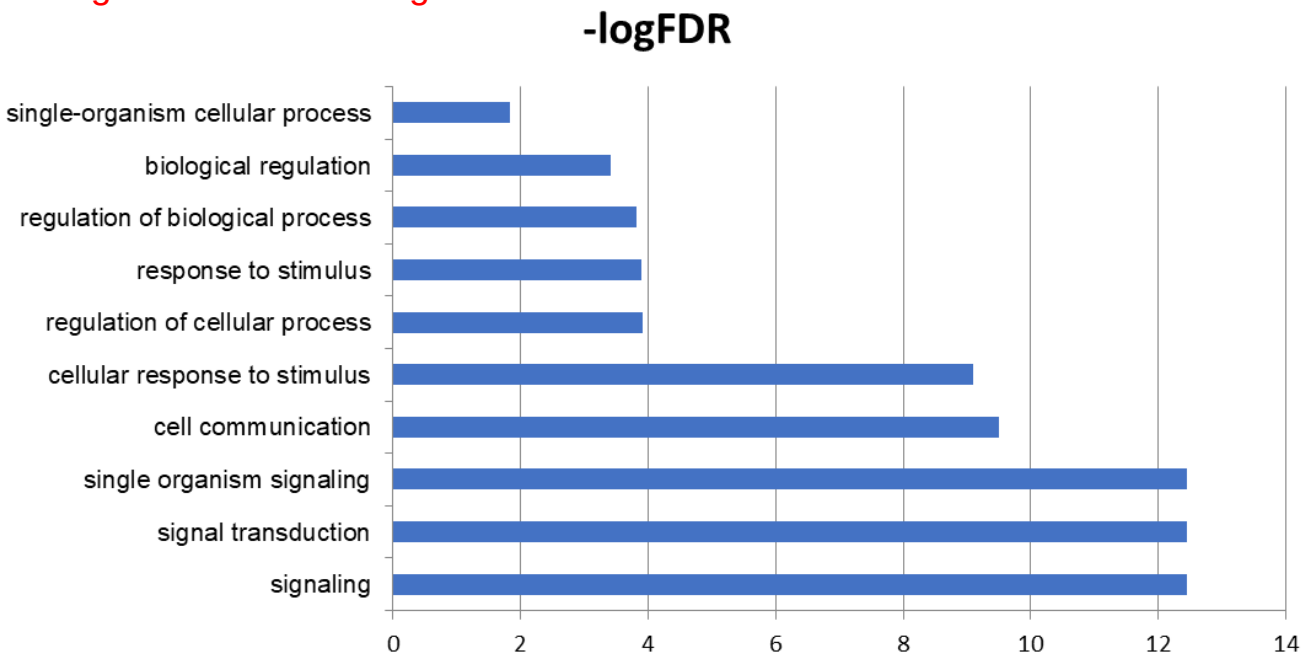

Molecular Function in Region II

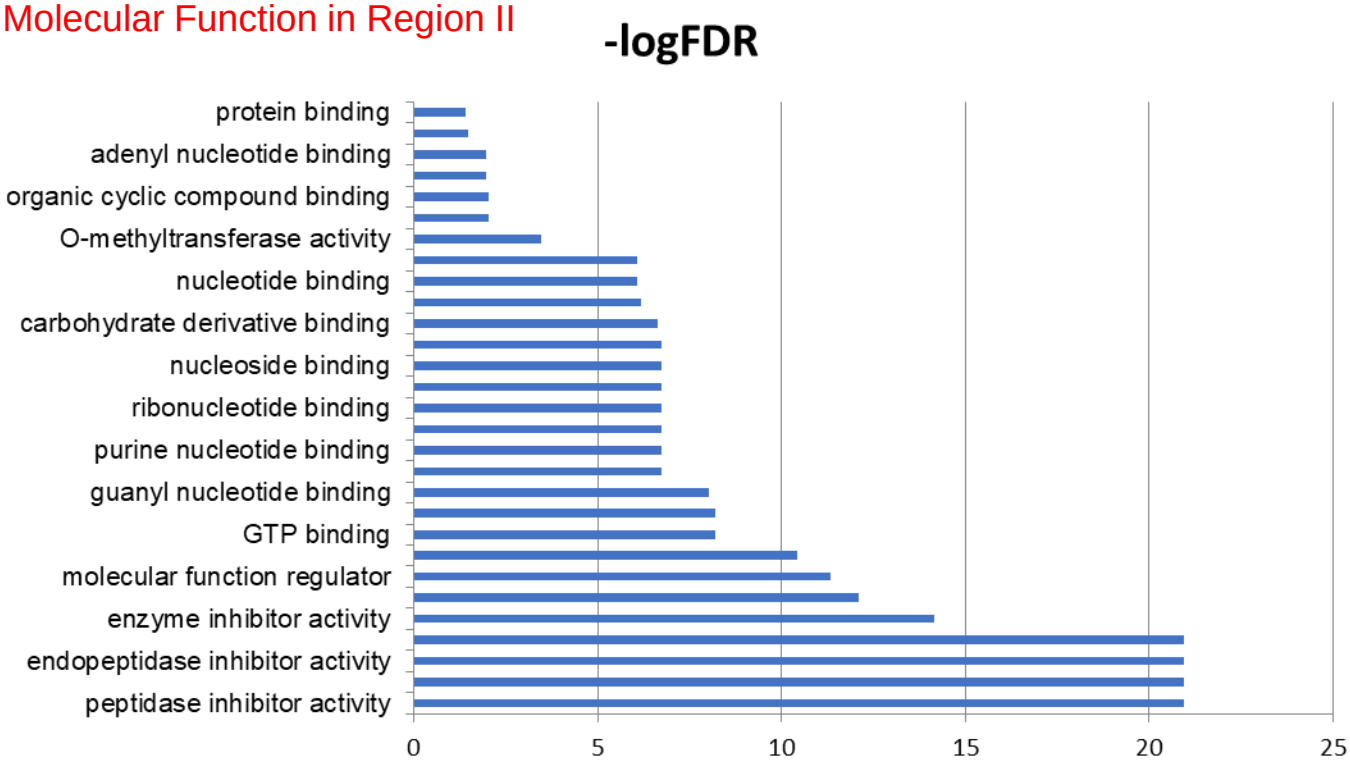

Biological Process in Region III

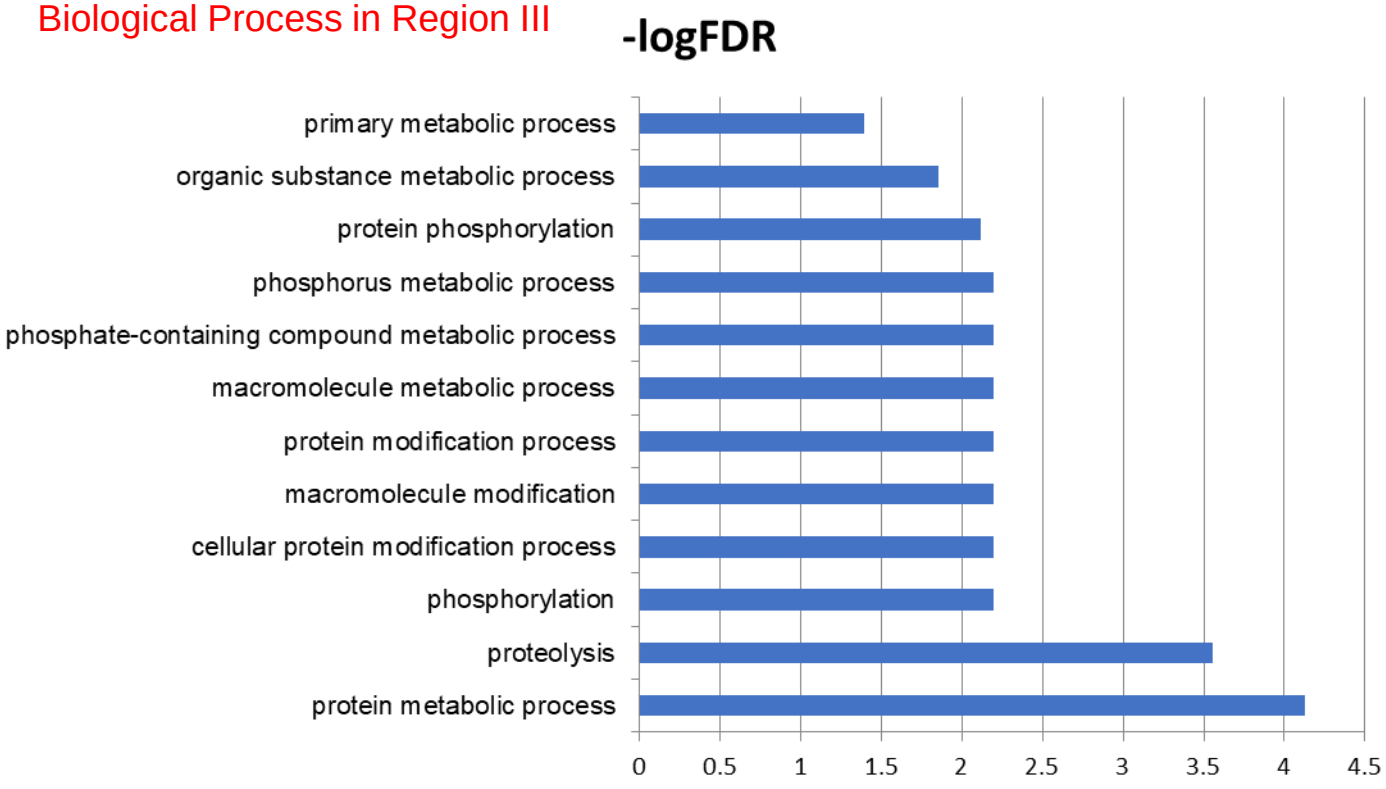

Molecular Function in Region III

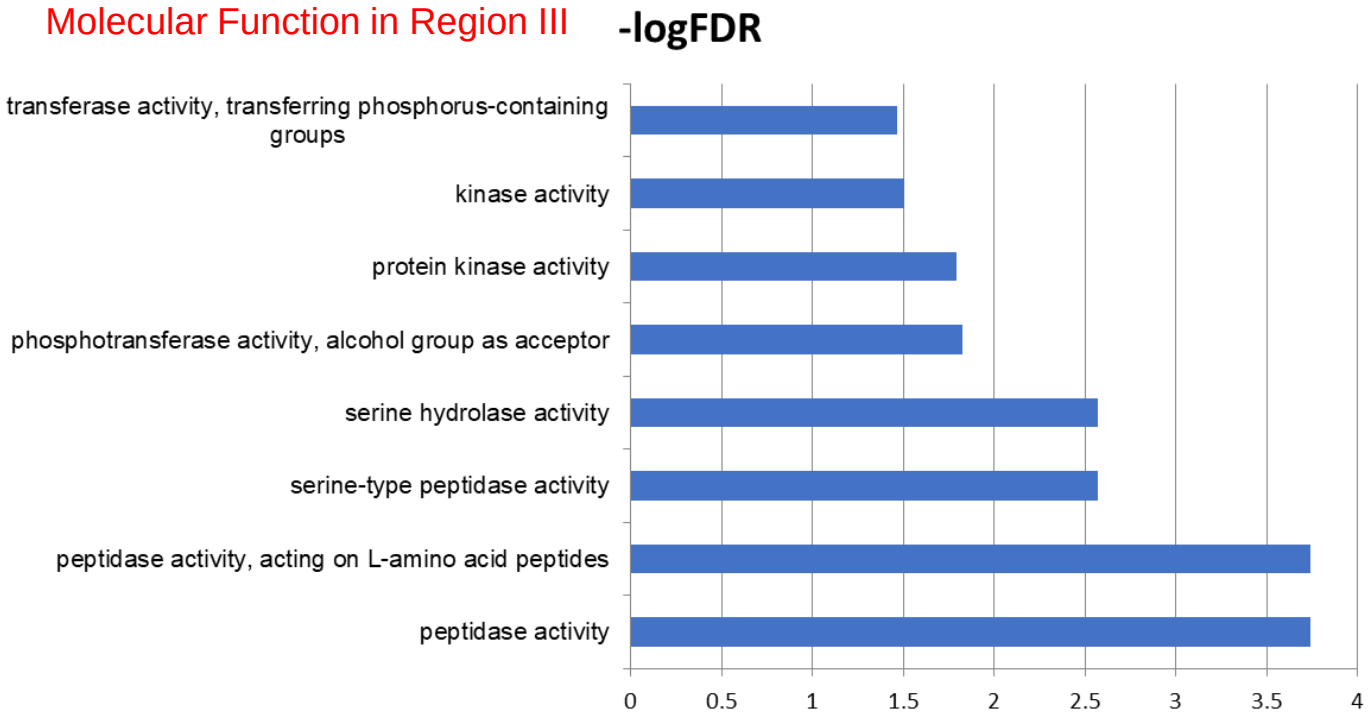

Biological Process in Region IV

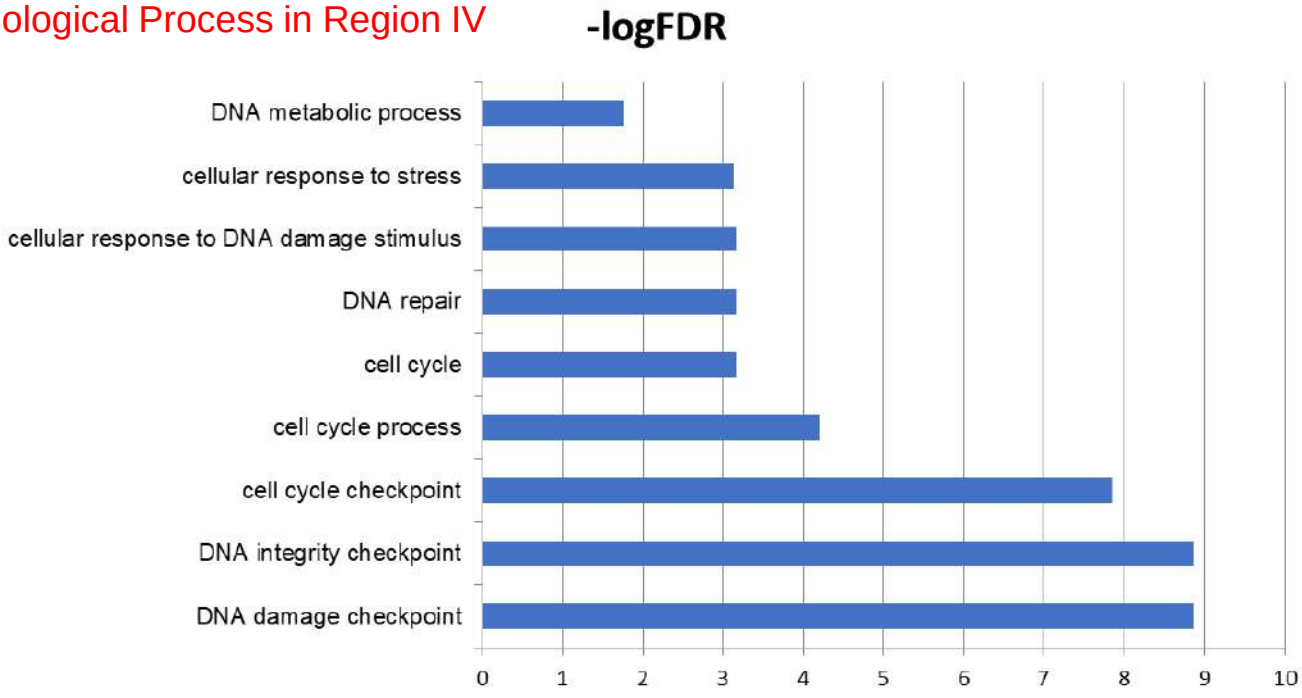

Molecular Function in Region IV

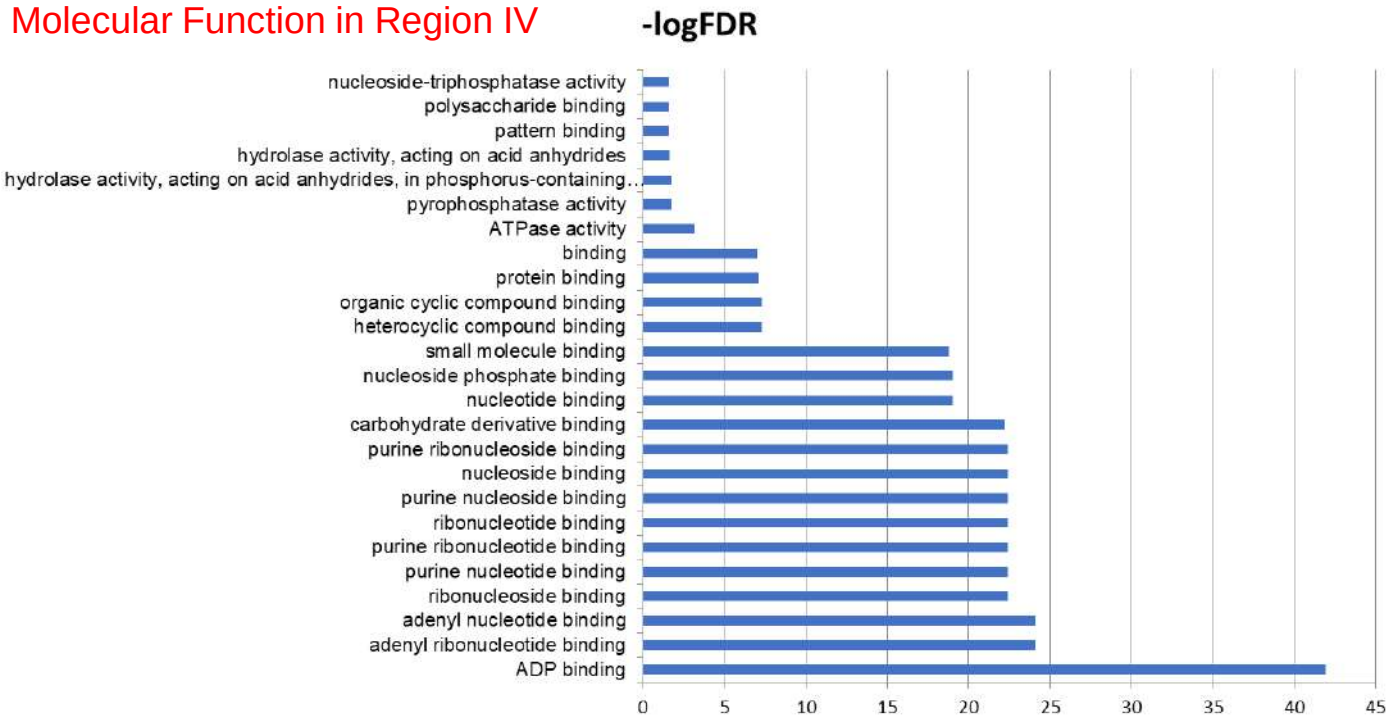

Biological Process in Region V

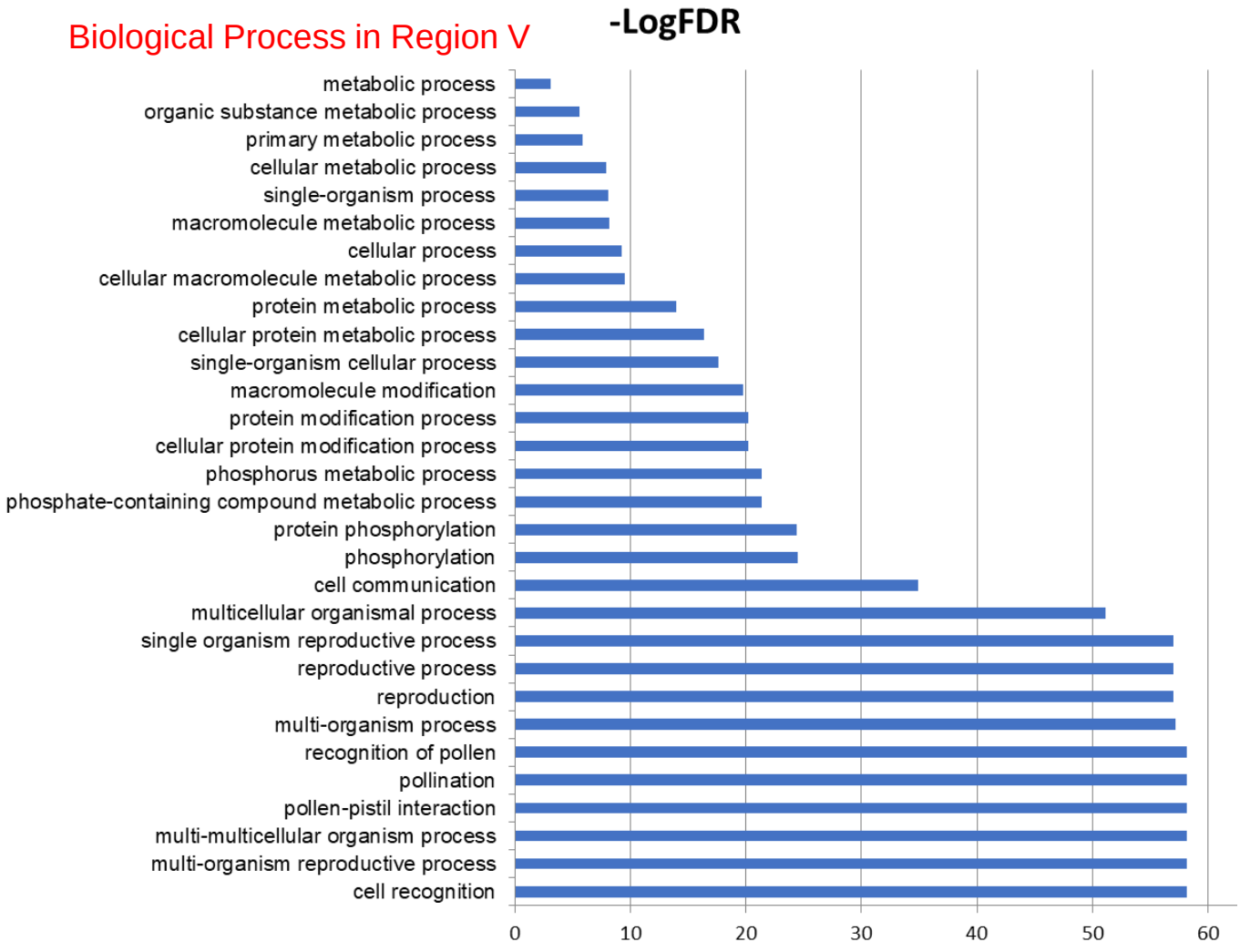

Molecular Function in Region V

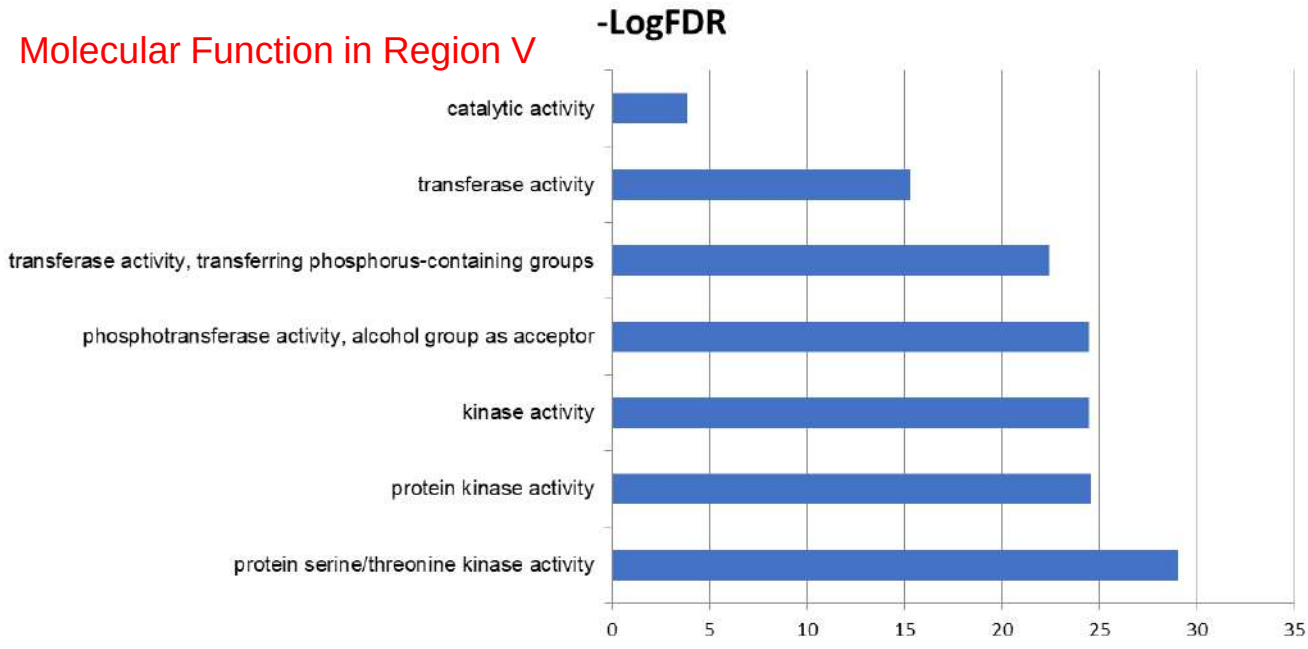

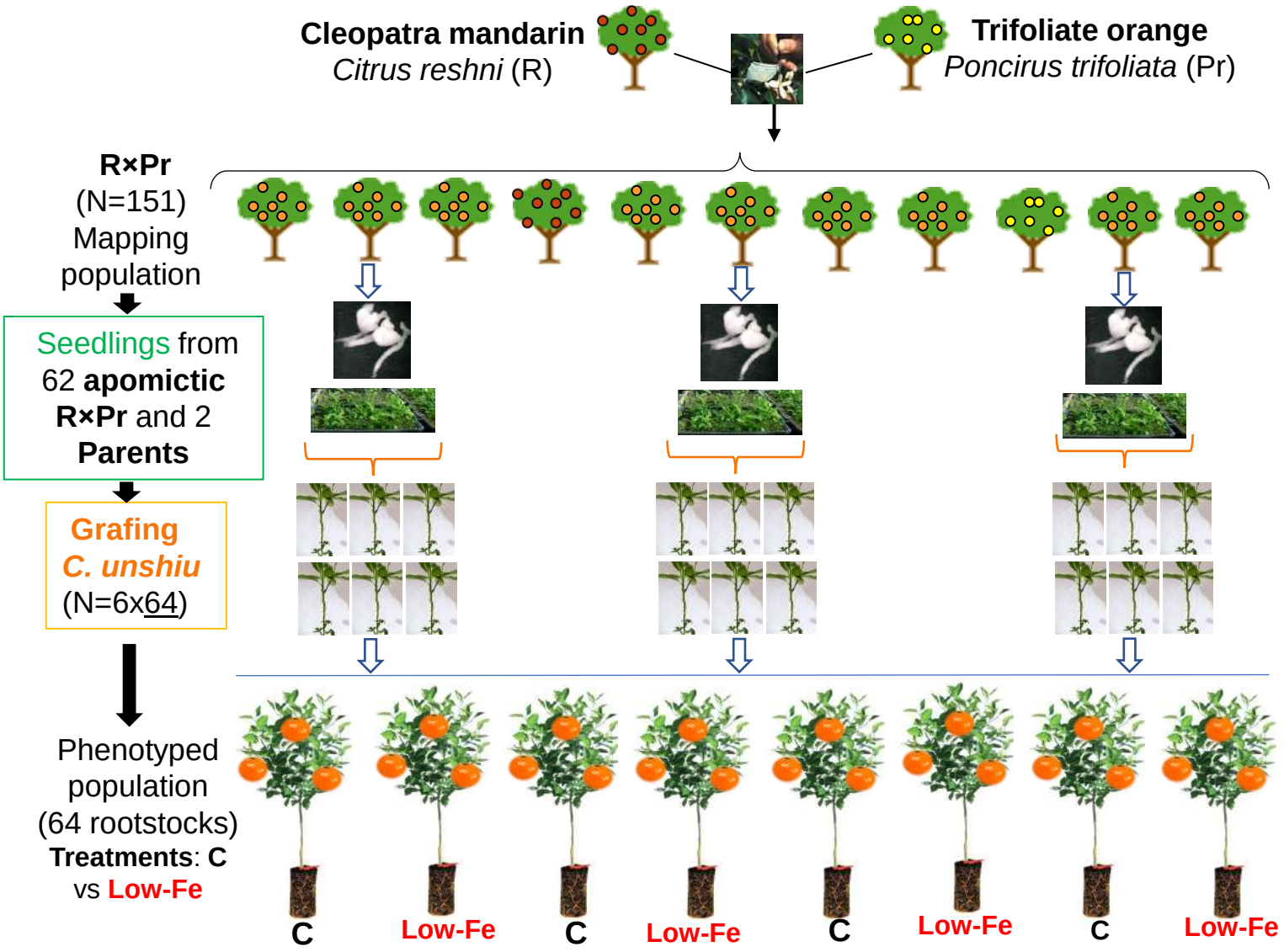
Cleopatra mandarin
Citrus reshni (R)
Trifoliate orange
Poncirus trifoliata (Pr)
R×Pr
(N=151)
Mapping
population
Seedlings from
62 apomictic
R×Pr and 2
Parents
Grafing
C. unshiu
(N=6x64)
Phenotyped
population
(64 rootstocks)
Treatments: C
vs Low-Fe
C
Low-Fe
C
Low-Fe
C
Low-Fe
C
Low-Fe

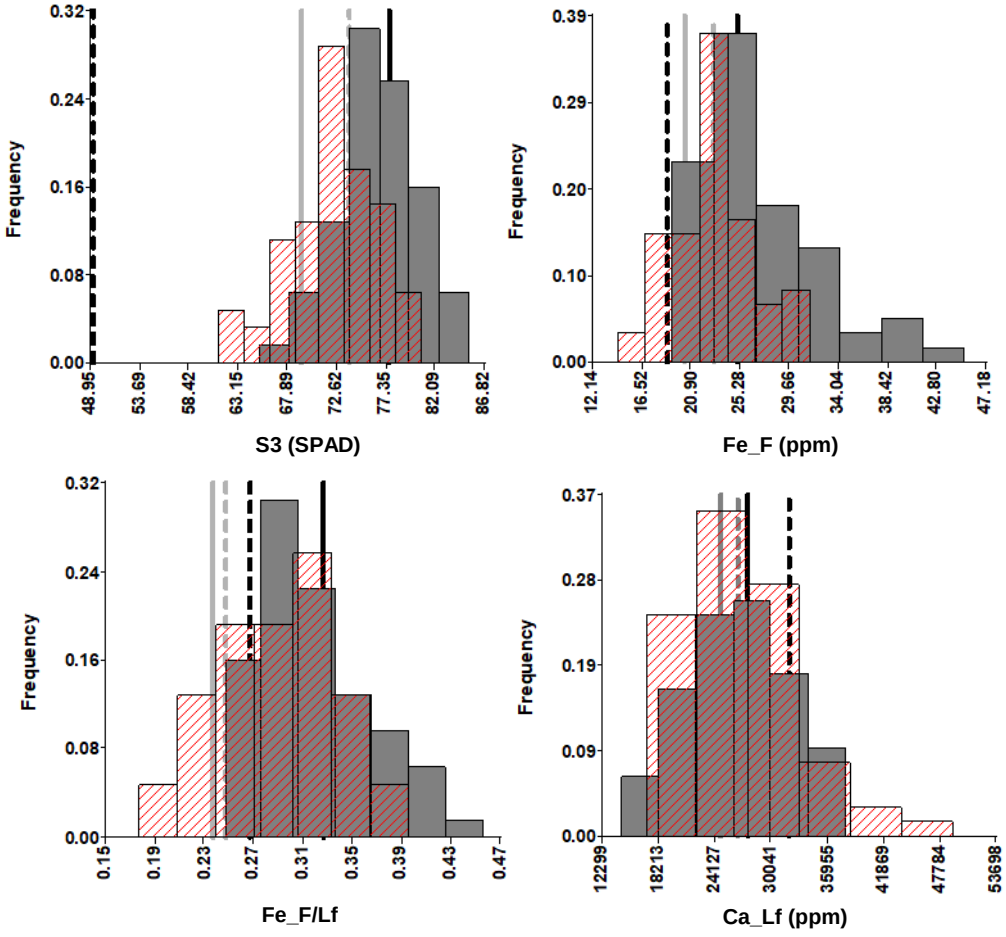
Frequency
0.32
0.24
0.16
0.08
0.00
48.95
53.69
58.42
63.15
67.89
72.62
77.35
82.09
86.82
S3 (SPAD)
Frequency
0.39
0.29
0.20
0.10
0.00
12.14
16.52
20.90
25.28
29.66
34.04
38.42
42.80
47.18
Fe_F (ppm)
Frequency
0.32
0.24
0.16
0.08
0.00
0.15
0.19
0.23
0.27
0.31
0.35
0.39
0.43
0.47
Fe_F/Lf
Frequency
0.37
0.28
0.19
0.09
0.00
12299
18213
24127
30041
35955
41869
47784
53698
Ca_Lf (ppm)

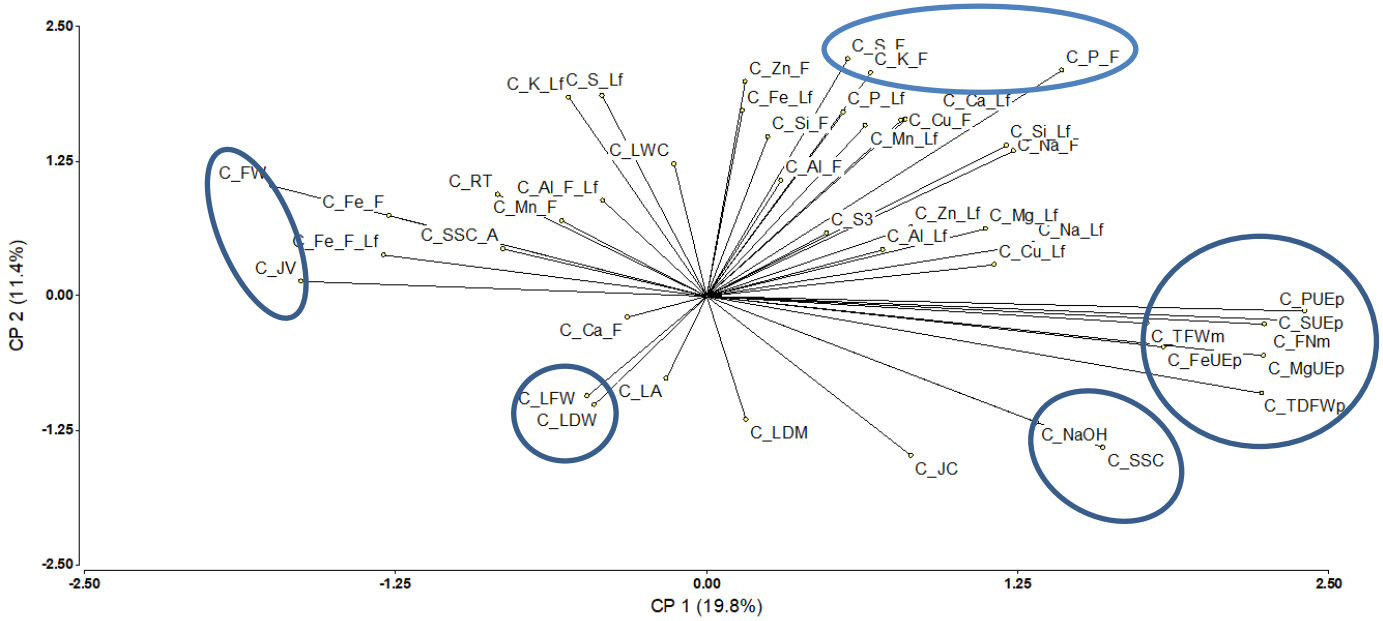
2.50
1.25
0.00
-1.25
-2.50
CP 2 (11.4%)
-2.50
-1.25
0.00
1.25
2.50
CP 1 (19.8%)
C_FW
C_Fe_F
C_Fe_F_Lf
C_JV
C_SSC_A
C_RT
C_Al_F_Lf
C_Mn_F
C_K_Lf
C_S_Lf
C_LWC
C_Zn_F
C_Fe_Lf
C_Si_F
C_S_F
C_K_F
C_P_Lf
C_Al_F
C_P_F
C_Ca_Lf
C_Cu_F
C_Mn_Lf
C_Si_Lf
C_Na_F
C_S3
C_Zn_Lf
C_Mg_Lf
C_Al_Lf
C_Na_Lf
C_Cu_Lf
C_Ca_F
C_LFW
C_LDW
C_LA
C_LDM
C_JC
C_NaOH
C_SSC
C_PUEp
C_SUEp
C_TFWm
C_FNm
C_FeUEp
C_MgUEp
C_TDFWp

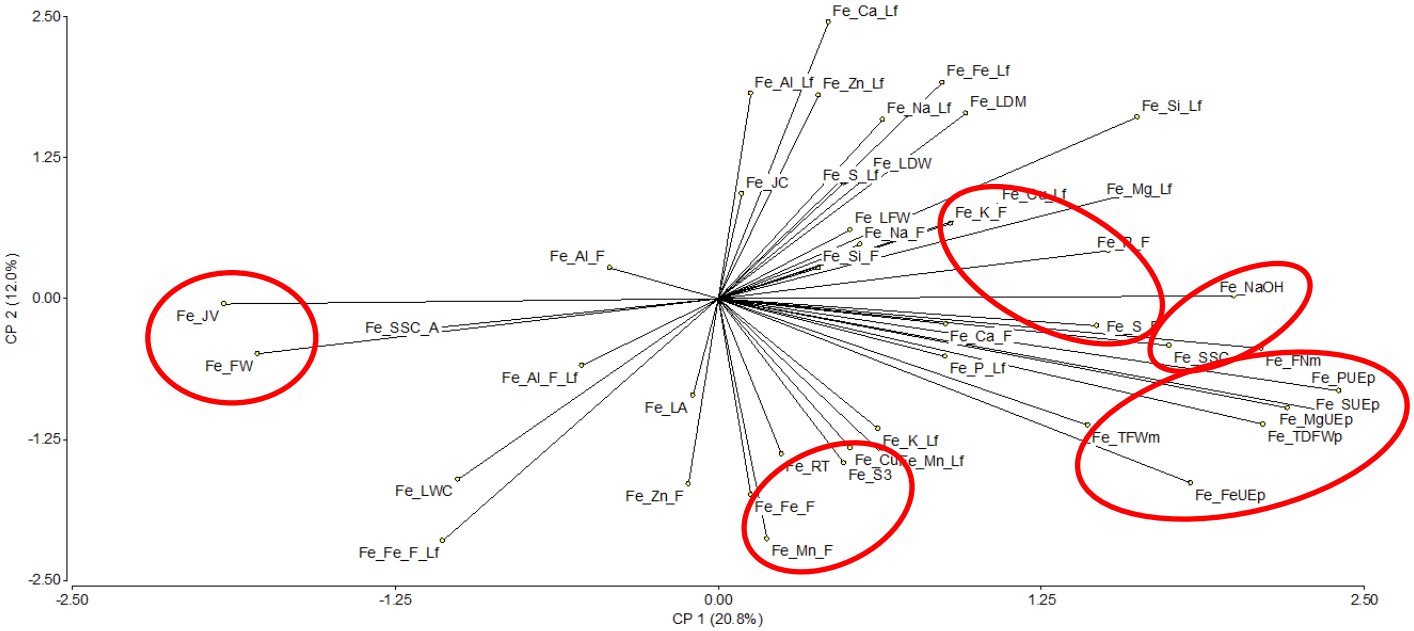
Fe_Ca_Lf
Fe_Al_Lf
Fe_Zn_Lf
Fe_Fe_Lf
Fe_Na_Lf
Fe_LDM
Fe_Si_Lf
Fe_LDW
Fe_JC
Fe_S_Lf
Fe_Mg_Lf
Fe_LFW
Fe_K_F
Fe_Na_F
Fe_Si_F
Fe_Al_F
Fe_NaOH
Fe_JV
Fe_SSC_A
Fe_Ca_F
Fe_FW
Fe_SSC
Fe_FNm
Fe_P_Lf
Fe_PUEp
Fe_SUEp
Fe_Al_F_Lf
Fe_MgUEp
Fe_LA
Fe_K_Lf
Fe_TFWm
Fe_TDFWp
Fe_RT
Fe_Cu
Fe_Mn_Lf
Fe_S3
Fe_LWC
Fe_Zn_F
Fe_FeUEp
Fe_Fe_F
Fe_Fe_F_Lf
Fe_Mn_F
2.50
1.25
0.00
-1.25
-2.50
CP 2 (12.0%)
-2.50
-1.25
0.00
1.25
2.50
CP 1 (20.8%)

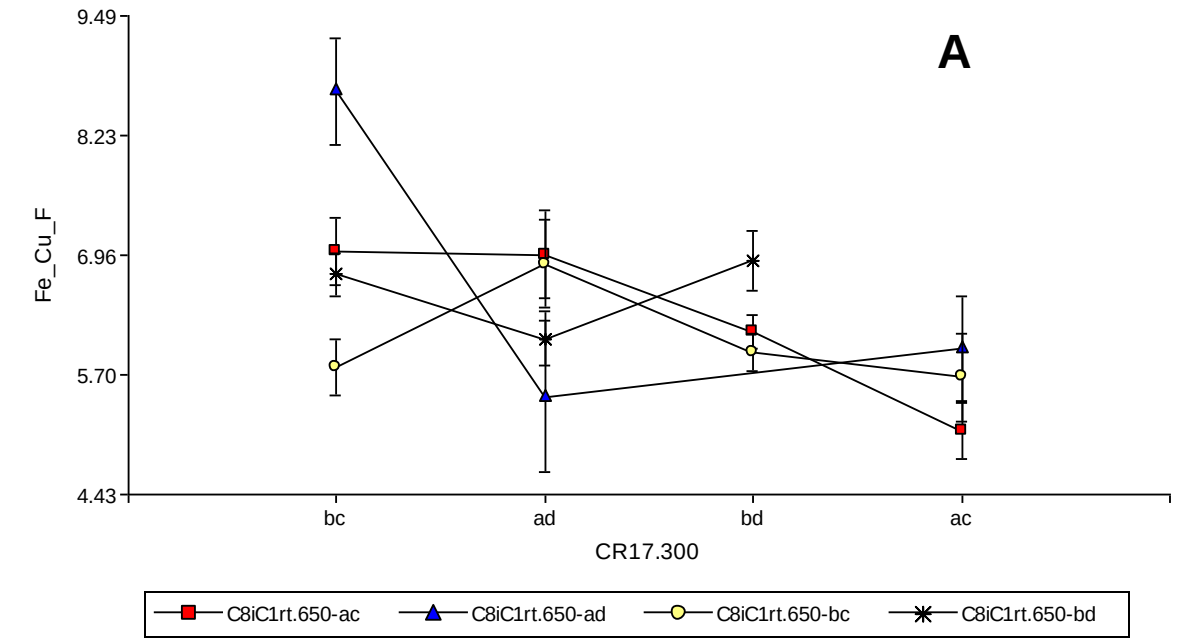
A
9.49
8.23
6.96
5.70
4.43
Fe_Cu_F
bc
ad
bd
ac
CR17.300
C8iC1rt.650-ac
C8iC1rt.650-ad
C8iC1rt.650-bc
C8iC1rt.650-bd

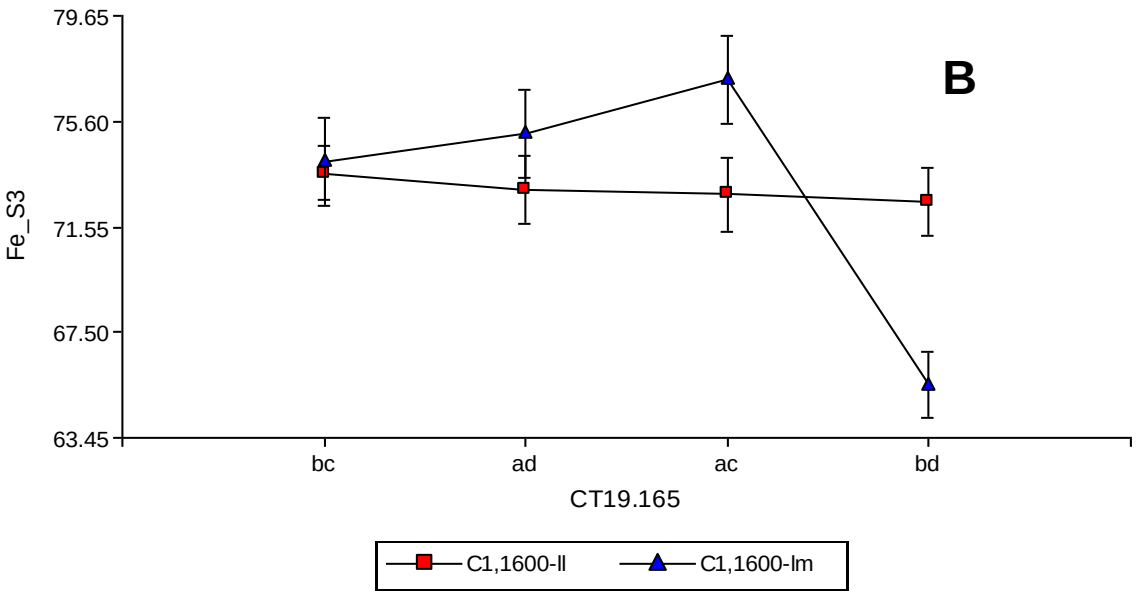
B
79.65
75.60
71.55
67.50
63.45
Fe_S3
bc
ad
ac
bd
CT19.165
C1,1600-ll
C1,1600-lm

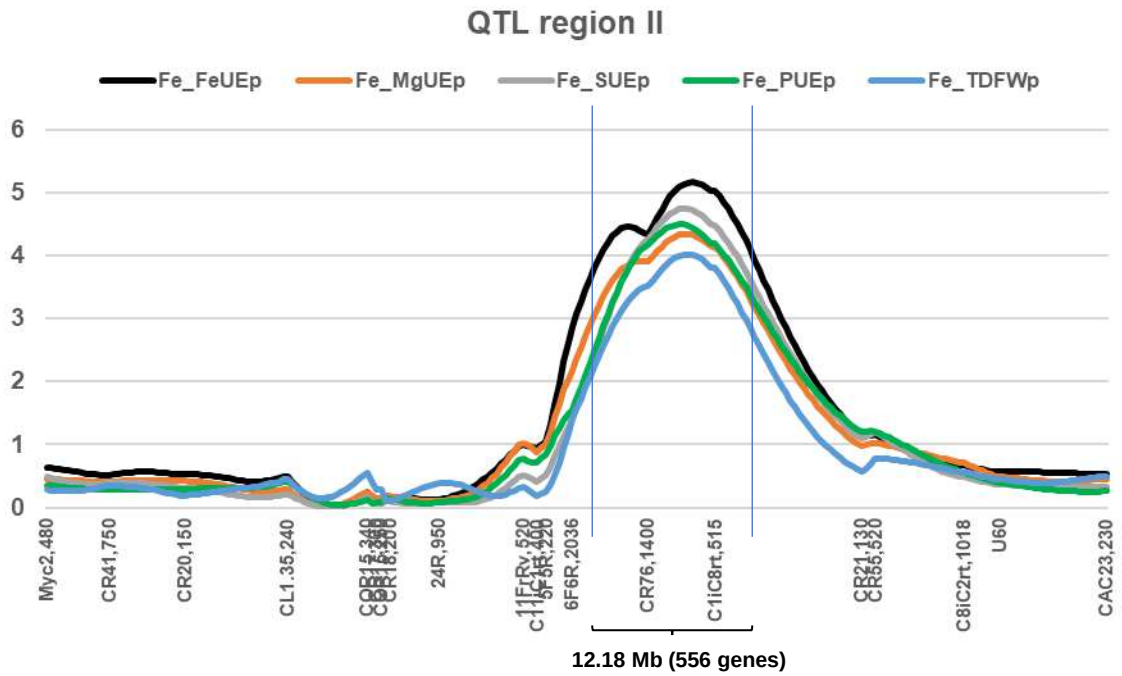
QTL region II
Fe_FeUEp
Fe_MgUEp
Fe_SUEp
Fe_PUEp
Fe_TDFWp
0
1
2
3
4
5
6
Myc2,480
CR41,750
CR20,150
CL1.35,240
24R,950
6F6R,2036
CR76,1400
C1iC8rt,515
CR21,130
C8iC2rt,1018
U60
CAC23,230
12.18 Mb (556 genes)

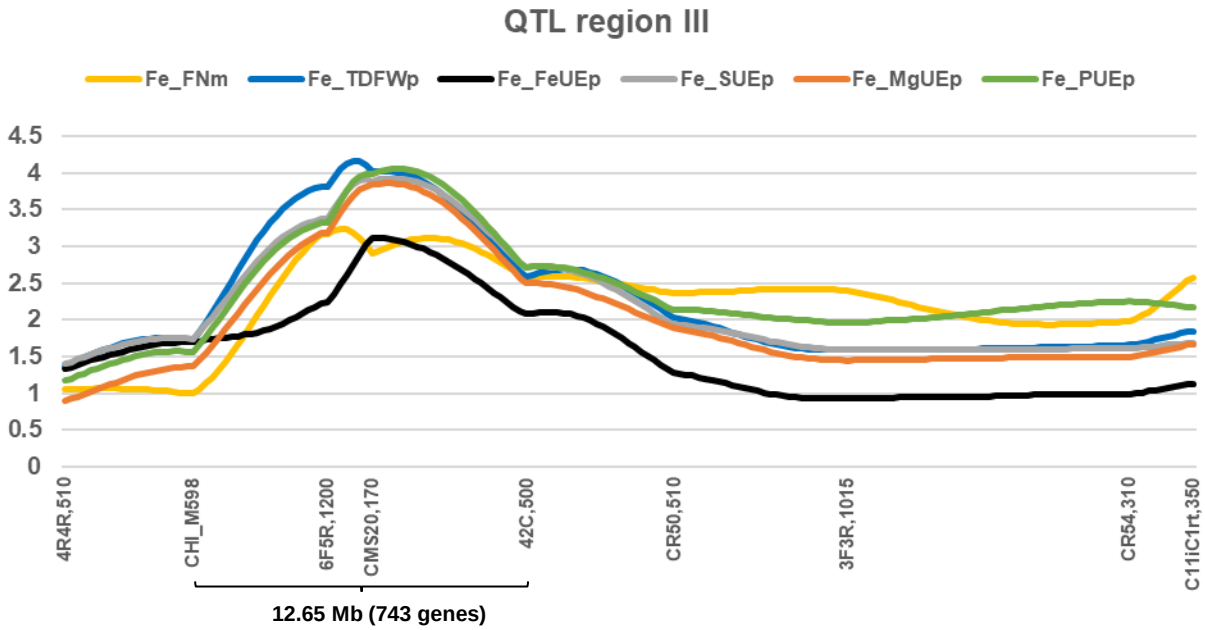
QTL region III
Fe_FNm
Fe_TDFWp
Fe_FeUEp
Fe_SUEp
Fe_MgUEp
Fe_PUEp
0
0.5
1
1.5
2
2.5
3
3.5
4
4.5
4R4R,510
CHI_M598
6F5R,1200
CMS20,170
42C,500
CR50,510
3F3R,1015
CR54,310
C11iC1rt,350
12.65 Mb (743 genes)

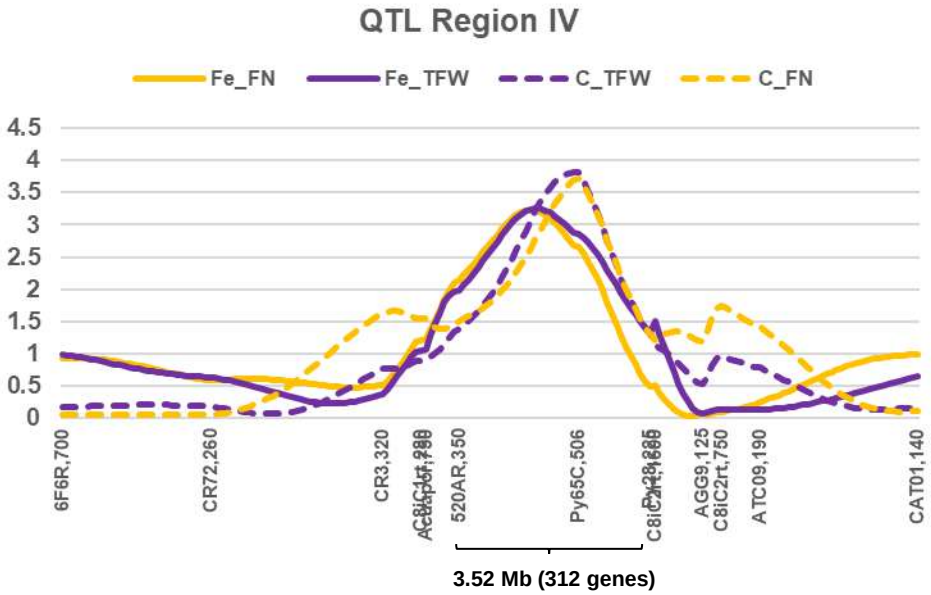
QTL Region IV
Fe_FN
Fe_TFW
C_TFW
C_FN
0
0.5
1
1.5
2
2.5
3
3.5
4
4.5
6F6R,700
CR72,260
CR3,320
520AR,350
Py65C,506
AGG9,125
C8iC2rt,750
ATC09,190
CAT01,140
3.52 Mb (312 genes)